

Award Accounts

The Chemical Society of Japan Award for Creative Work for 2002

Multi-Mode Molecular Switching Properties and Functions of Azo-Conjugated Metal Complexes

Hiroshi Nishihara

Department of Chemistry, School of Science, The University of Tokyo, Hongo, Tokyo 113-0033

Received September 18, 2003; E-mail: nishihara@chem.s.u-tokyo.ac.jp

Recent studies on the azo-group-combined photochromic metal complexes are reviewed. These studies show unique *trans*–*cis* isomerization behaviors that have not been observed in regular organic azobenzenes. In the case of azobenzene-bound bis(terpyridine) complexes of transition metals, photoisomerization behavior depends strongly on the central metals, counterions, and solvents. Rh and Co complexes undergo photoisomerization smoothly, but the isomerization of Ru and Fe complexes is substantially retarded due to the energy transfer from the π – π^* excited state to the MLCT transition. The photoluminescence property of an azobenzene-attached Pt complex is switched by photoisomerization of the azo moiety. Tris(azobenzene-bound bipyridine)cobalt undergoes reversible *trans*–*cis* isomerization using a combination of the $\text{Co}^{\text{III}}/\text{Co}^{\text{II}}$ redox change and a single UV light source exciting the π – π^* transition. The *trans*–*cis* conversion yield is higher for the meta isomer (with respect to the position of the azo group against the pyridyl group) than for the para isomer. The *trans*–*cis* photoisomerization behavior of a 6,6'-dimethyl-substituted azobenzene-bipyridine ligand is synchronized with coordination of the bipyridine moiety to copper, and the *trans*/*cis* isomerization can be controlled reversibly through $\text{Cu}^{\text{II}}/\text{Cu}^{\text{I}}$ redox and a single UV light irradiation. Photoreaction of azoferrocene occurs not only by UV-light irradiation but also by green light irradiation that excites the MLCT transition. 3-Ferrocenylazobenzene undergoes reversible *trans*–*cis* isomerization using a single green light source and the $\text{Fe}^{\text{III}}/\text{Fe}^{\text{II}}$ redox change. Azo-conjugated metalladithiolenes of Ni^{II} , Pd^{II} , and Pt^{II} with diphenylphosphinoethane as a co-ligand show facile photoisomerization. The energy of the reversible *trans*-to-*cis* photoisomerization is considerably lower than that of azobenzene. The thermal stability of the *cis* form is, however, much higher than that of the organic azobenzene derivatives showing similar low-energy *trans*-to-*cis* photoisomerization. A novel proton response of the azo group occurs, and the combination of photoisomerization and protonation leads to a novel proton-catalyzed *cis*-to-*trans* isomerization. These results indicate that several kinds of multi-photo-functionalities can be realized for the azo-conjugated transition metal complexes by tuning the interaction between the azo moiety and the metal complex unit.

In the forthcoming technology related to molecular-based electronic and photonic devices, there is need of a methodology to handle electrons in a single molecule by applying outer stimuli without restraint; for this methodology, an appropriate molecular design will be one of the most important factors.¹ Electrons in d-orbitals of transition metals and π -orbitals of conjugated π -systems can be easily managed because of the modest energy levels of both the d- and π -orbitals. A combination of transition metals and π -conjugated systems with d– π electronic interaction might thus be used to realize novel optical, electronic, and magnetic properties and functions. From this viewpoint, we have developed a series of d– π conjugated metal complex systems, π -conjugated organometallic conducting polymers such as metallacycle polymers,^{2,3} multiply conjugated redox nuclei systems such as oligo(ferrocene-1,1'-diyl)s,⁴ intelligent metal complex molecules such as the ferrocene–quinone donor–acceptor conjugated molecules,^{5,6} and metal nanoparticles modified with redox-active species.⁷ In this review, we focus on one of the conjugated metal complex systems that can respond

to external perturbation, the so-called “azo-conjugated metal complex” system.

Photochromic molecules that have a structure—and therefore an electronic structure and color—that changes reversibly by photoirradiation have been attracting much attention recently because of their possible applications in the area of photon-mode high-density information storage and photo-switching devices.^{8–10} Azobenzene is one of the representative photochromic molecules with two geometric isomers, a *trans* form and a *cis* form.^{11–14} The *trans*-to-*cis* isomerization occurs by irradiation of the π – π^* band with UV light, and the *cis*-to-*trans* isomerization proceeds by excitation of the n– π^* band with blue-light irradiation or by heating, because the *trans* form is thermodynamically more stable than the *cis* form. By combining transition metal complexes with the azo group, many functional molecules might be produced by the fusion of the two independently functional molecular units. There are two interesting questions in regard to the azo-conjugated transition metal complexes. First, what are the effects of metal complex units

on the isomerization? And second, what are the changes in the physical properties of metal complex units caused by isomerization? In our effort to provide general answers to these questions, we have studied several kinds of metal complexes simultaneously. It should be noted that several metal complexes including azobenzene and related compounds as building blocks have been reported by other groups.^{15–20} In our studies, we have found several new properties of such complexes and their multi-mode isomerization; we describe these findings in this review.

1. Azobenzene-Attached Bis(terpyridine)metal Complexes with Strong Dependencies of the Isomerization Behavior on the Central Metal, Counterion, and Solvent

Bis(2,2':6',2''-terpyridine) complexes with hexa-coordinated octahedral conformations have received continuous attention because they have no geometric isomers, they can incorporate various kinds of metals, and they can afford pliant systems for fundamental investigations into the electronic interaction between metal centers, photoinduced energy, and electron transfer.^{21–30} We have employed four kinds of metals; Fe, Co, Ru, and Rh (Chart 1), for the study of the photoisomerization behavior of metal complexes with azobenzene-attached terpyridine and bis(terpyridine) ligands, **1** and **2**, because the redox and optical properties of the complexes are highly reliant on the metal center. It has been demonstrated that the bis(terpyri-

dine) complexes of Fe, Co, and Ru show reversible redox behavior, that the Fe^{II} and Ru^{II} complexes have a strong MLCT band in the visible region, and that the Ru(II) complex exhibits effective photoluminescence.

The dependences of the photoisomerization behavior on the metal center and its oxidation state are significant. As for the Fe^{II} and Ru^{II} complexes, **3–5**, photoisomerization using UV light irradiation exciting the π – π^* band of the azobenzene moiety in the *trans* form is totally inhibited, and the photoluminescence property of the Ru^{II} complex is quenched.^{31–33} In the transient absorption spectra of the Ru complex, **5**, very fast bleaching of the Ru MLCT band at 500 nm occurs, implying that the photoisomerization behavior is depressed in response to the energy transfer from the azobenzene unit to the complex unit, as shown in Fig. 1.³² Similar bleaching behavior was observed for the Fe^{II} complex, **3**.³³ These results indicate that the *trans*-to-*cis* photoisomerization behavior of polypyridine complexes having a strong MLCT band, the energy of which is lower than that of the azo π – π^* band, is depressed by the energy transfer pathway.

In contrast to the group 8 metal (Fe, Ru) complexes, the group 9 metal (Co, Rh) complexes undergo significant *trans*-to-*cis* photoisomerization.^{32–34} In the case of the Rh complexes, we investigated the difference in photoisomerization between the mononuclear and dinuclear forms, and the effects of counterion and solvent on the isomerization. Among the mononu-

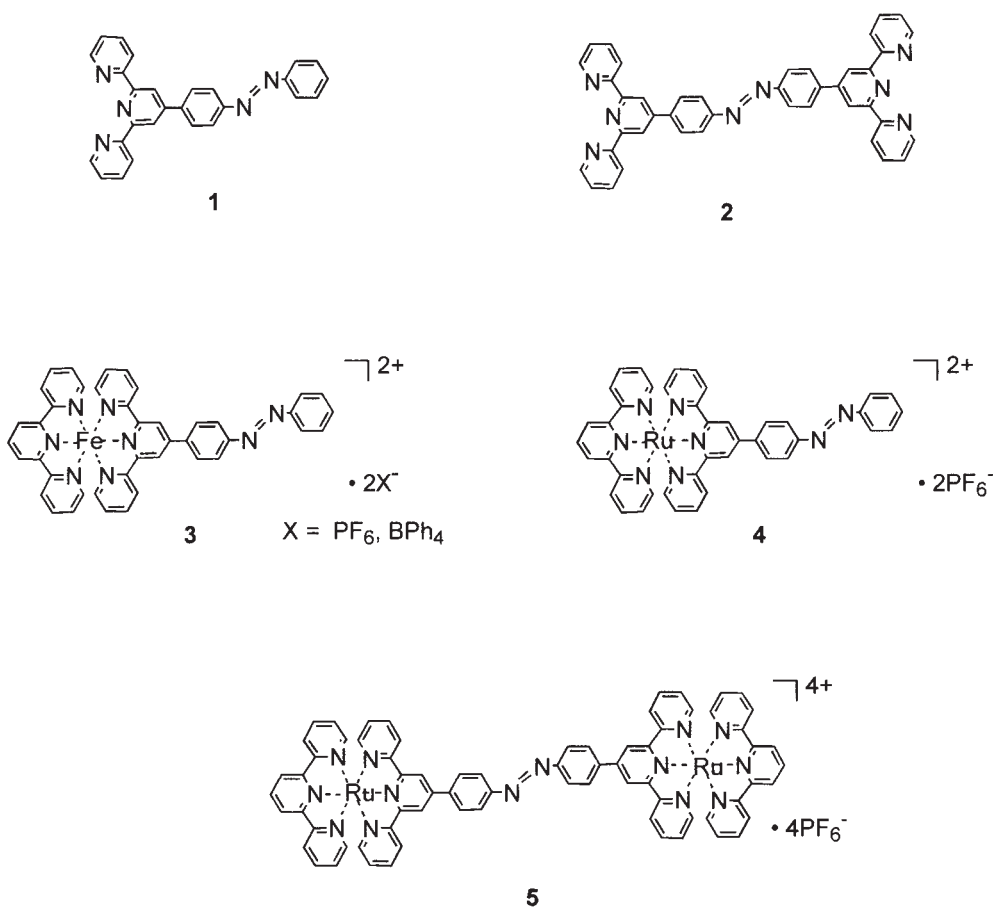


Chart 1.

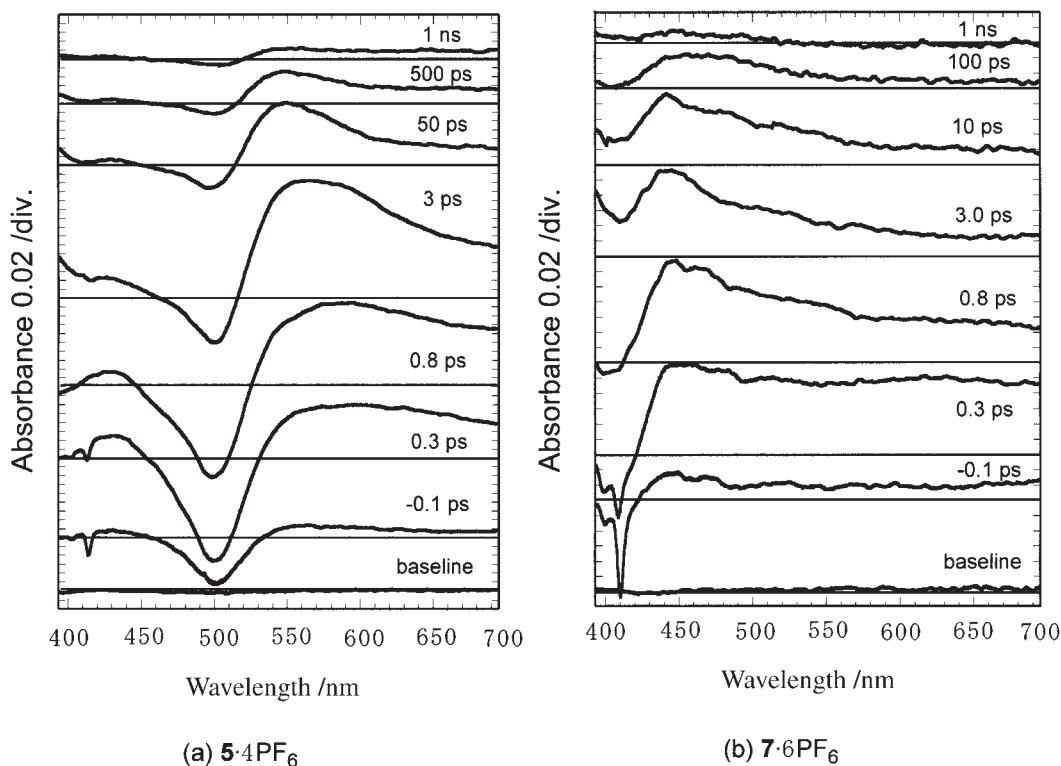


Fig. 1. Transient absorption spectra of **5·4PF₆** (a) and **7·6PF₆** (b) in MeCN, excited by the second harmonic (360 nm) of the fundamental (center wavelength 720 nm, pulse width ~ 200 fs FWHM). Each spectrum was obtained by averaging over 200 pulses (Reprinted with permission from Ref. 32).

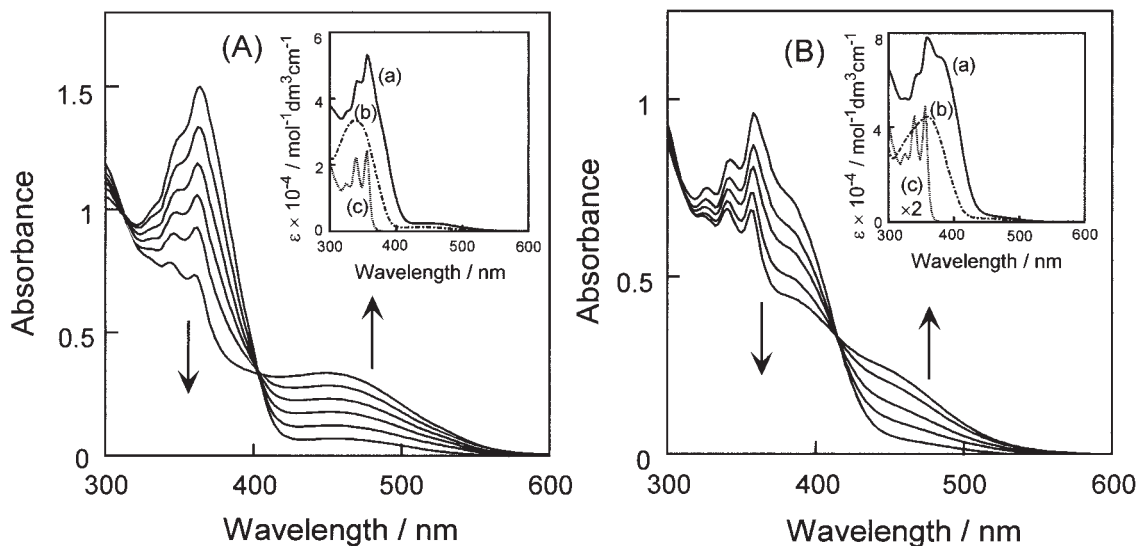


Fig. 2. (A) UV-vis spectral change of **6·3PF₆** (2.8×10^{-4} mol dm⁻³) in DMSO upon irradiation at 366 nm for 5 min. Inset: the spectra of **6·3PF₆** (a), **1** (b), and [Rh(tpy)₂](PF₆)₃ (c). (B) UV-vis spectral change of **7·6PF₆** (1.1×10^{-4} mol dm⁻³) in PC upon irradiation at 366 nm for 40 min. Inset: the spectra of **7·6PF₆** (a), **2** (b), and [Rh(tpy)₂](PF₆)₃ (c) (Reprinted with permission from Ref. 32).

clear and dinuclear Rh complexes, **6** and **7** show significant UV-vis spectral changes attributable to the *trans*-to-*cis* isomerization, including a decrease in the absorbance of the π - π^* band and an increase in the longer wavelength band ascribable to the n - π^* transition on 366-nm light irradiation (Fig. 2, Chart 2). The *cis* form formation causes the ¹H NMR spectral change as a higher magnetic field shift of the aromatic ring

protons by changing the ring current effects of the azobenzene group.³⁵ In the IR spectra of the isolated *cis* complexes, a weak peak due to the N=N stretching mode, which is IR-inactive in *trans*-complexes due to their inversion symmetry,³⁶⁻³⁸ appears at ca. 1530 cm⁻¹. Cyclic voltammetry of the *trans* form of **7·6BF₄** in Bu₄NBF₄-MeCN shows an irreversible Rh^{III}/Rh^I reduction wave at -1.01 V vs ferrocenium/ferrocene (Fc⁺/

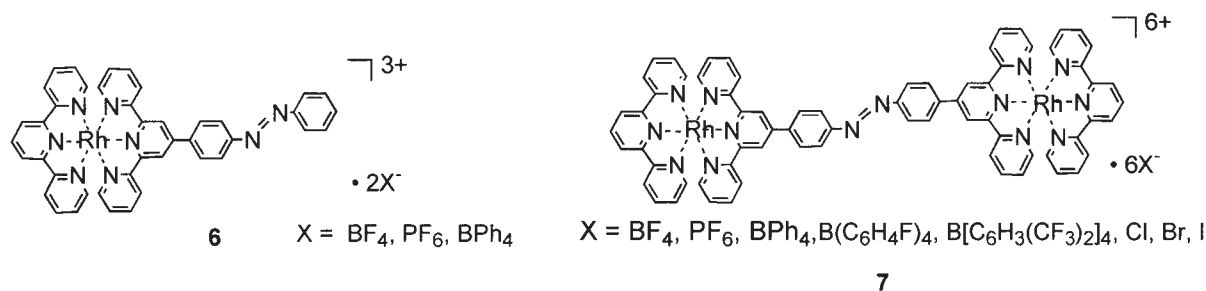


Chart 2.

Table 1. Quantum Yields of Mononuclear and Dinuclear Rh Complexes Dependent on Various Solvents and Counterions

Solvent	Dielectric constant ^{a)}	Viscosity ^{a)} ($\eta/\text{mPa s}$)	$10^3 \Phi_{t \rightarrow c}$					
			7 ·6BF ₄	7 ·6PF ₆	7 ·6BPh ₄	6 ·3BF ₄	6 ·3PF ₆	6 ·3BPh ₄
PhCN	25.9	1.27	0.29	b)	b)	0.34	0.062	3.9
MeCN	36.6	0.369	b)	b)	5.7	0.016	0.011	5.1
DMF	38.3	1.794	2.7	2.9	2.3	3.4	3.9	5.5
DMA	38.9	1.96	4.2	4.0	4.2	3.5	4.4	5.4
DMSO	47.2	1.99	1.9	1.6	2.1	0.58	1.6	3.3
PC	68.8	2.53	0.042	b)	0.25	0.052	0.11	1.5

a) D. R. Lide, "CRC Handbook of Chemistry and Physics," 79th ed, CRC Press (1998). b) No significant photoisomerization behavior was observed ($\Phi_{t \rightarrow c} < 10^{-6}$).

Fc), which shifts to -1.09 V in the *cis* form, because the electron-withdrawing effect of the azo group is smaller in the *cis* form than in the *trans* form.

It is noteworthy that the *cis*-to-*trans* photoisomerization, upon excitation of the azo $n \rightarrow \pi^*$ transition by 430-nm light irradiation, does not occur for any of the mononuclear and dinuclear Rh complexes, whereas the thermal isomerization proceeds at a much slower rate than that of the free ligands.³²

In this series of complexes, the metal complex site is large and has a positive charge, and thus the effects of counterion on the photoisomerization rate are intriguing. We measured the quantum yields of the *trans*-to-*cis* photoisomerization—i.e., the $\Phi_{t \rightarrow c}$ values—for **6** and **7** with various counterions; selected results are listed in Table 1. The $\Phi_{t \rightarrow c}$ values are much smaller than those of organic azobenzenes,^{39–47} and show strong dependence on the counterions and solvents.³² The photoisomerization of a dinuclear complex, **7**·6BPh₄, proceeds more efficiently than that of **7**·6PF₆ or **7**·6BF₄. **7**·6BPh₄ is subject to *trans*-to-*cis* photoisomerization even in the KBr matrix, in which the free ligand does not show significant isomerization. One should note that the ion-pairing ability of the counterions contributes to the apparent rotor volume of the complexes for the isomerization. The electrostatic interaction between the complex cation and the counter anion, evaluated based on the ion-pairing peak distribution and the intensities of ESI mass spectra, is weaker for large BPh₄[−] than for small BF₄[−] and PF₆[−], for which the order is consistent with the tendency of $\Phi_{t \rightarrow c}$. This phenomenon can be explained if the anion with the lower ion-pairing ability reduces the apparent rotor volume for the isomerization, leading to a more facile isomerization. It is notable that the mononuclear complex, **6**, shows a small dependence of $\Phi_{t \rightarrow c}$ on the counterion. It would be expected that the counterion of **6** would not interact with the neu-

tral azobenzene moiety, and that the counterion would not interfere with the motion of the azobenzene moiety.

The behavior of the femtosecond transient absorption spectra of the Rh complex **7**·6PF₆ shown in Fig. 1b is similar to that of organic azobenzenes; at first a very broad $S_n \leftarrow S_2$ ($\pi \rightarrow \pi^*$ state) absorption band at ca. 500 nm (within 1 ps) appears and this decays rapidly.³² Next, an intense $S_n \leftarrow S_1$ ($n \rightarrow \pi^*$ state) absorption band at ca. 450 nm (within 2 ps) appears. The lifetime of the S_2 or S_1 state and the decay dynamics of the complexes are similar to those of organic azobenzenes,^{48–51} in which the *trans*-to-*cis* photoisomerization is believed to occur from the S_1 state. Our findings indicate that photoisomerization of **7** occurs from the S_1 state.

For the Co^{II} complexes, **8** and **9** (Chart 3), *trans*-to-*cis* photoisomerization is observed in propylene carbonate (PC) and DMSO, and less significantly in MeCN, upon irradiation with 366-nm light, as shown in Fig. 3.³³ The photo-products could be isolated by precipitation from PC solution by adding 1,4-dioxane; these products were characterized by IR spectroscopy for **9**·4PF₆. The peak ascribed to N=N stretching of the *cis* form appeared at 1534 cm^{-1} .^{36–38} The $\Phi_{t \rightarrow c}$ values of Co complexes for *trans*-to-*cis* photoisomerization are listed in Table 2. There are two characteristic features distinguishing these yields from those of the Rh complexes:³² (1) the $\Phi_{t \rightarrow c}$ of the Co complexes is much smaller; (2) the counterion effect is less evident in the Co complexes. The latter feature is probably attributable to the facts that the Rh complex cation is trivalent, that is has a greater charge, and that is has more counterions.

In contrast to the Rh^{III} complexes, the Co^{II} complexes undergo *cis*-to-*trans* isomerization in PC by both photoirradiation with visible light (435 nm) and heat, indicating that reversible *trans*-*cis* isomerization occurs. There is no counterion effect on the *cis*-to-*trans* photoisomerization.

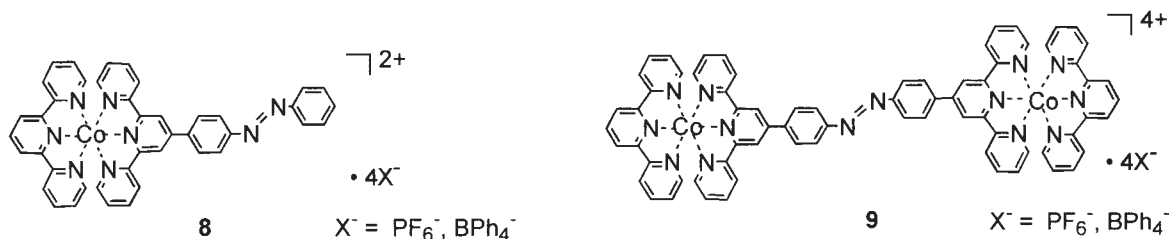


Chart 3.

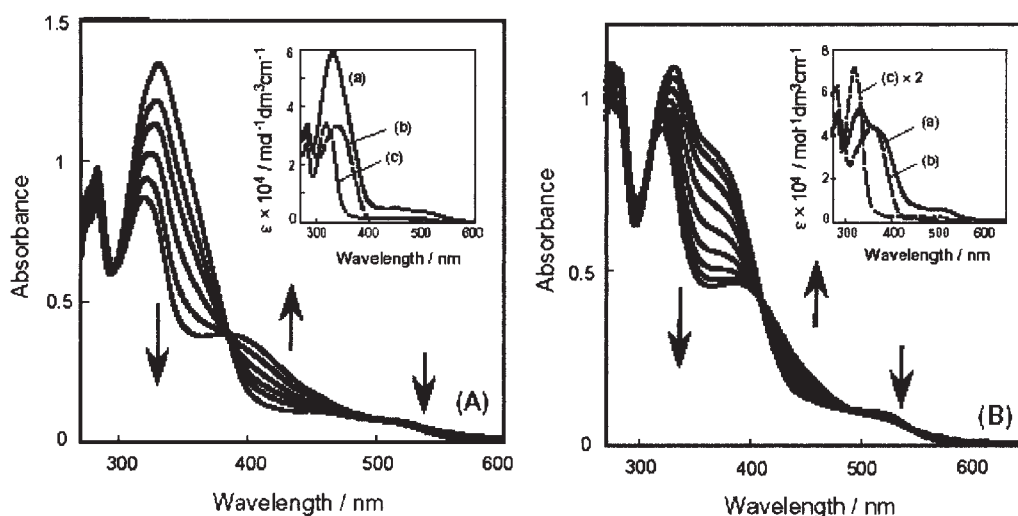


Fig. 3. (A) UV-vis spectral change of $8 \cdot 2\text{BPh}_4$ ($2.2 \times 10^{-5} \text{ mol dm}^{-3}$) in PC upon irradiation at 366 nm for 40 min. Inset: the spectra of $8 \cdot 2\text{PF}_6$ (a), **1** (b), and $[\text{Co}(\text{tpy})_2](\text{PF}_6)_2$ (c). (B) UV-vis spectral change of $9 \cdot 4\text{BPh}_4$ ($1.8 \times 10^{-5} \text{ mol dm}^{-3}$) in PC upon irradiation at 366 nm for 1 h. Inset: the spectra of $9 \cdot 4\text{PF}_6$ (a), **2** (b), and $[\text{Co}(\text{tpy})_2](\text{PF}_6)_2$ (c) (Reprinted with permission from Ref. 33).

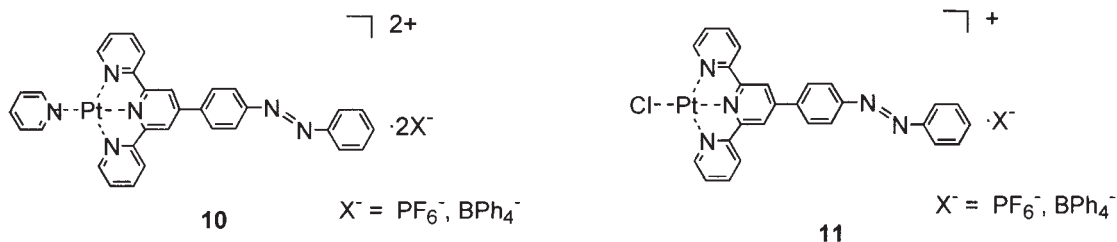


Chart 4.

Table 2. *trans*-to-*cis* Photoisomerization Quantum Yields ($\Phi_{t \rightarrow c}$) of the Co Complexes

Solvent	$10^4 \Phi_{t \rightarrow c}$			
	$8 \cdot 2\text{PF}_6$	$8 \cdot 2\text{BPh}_4$	$9 \cdot 4\text{PF}_6$	$9 \cdot 4\text{BPh}_4$
MeCN	<1	<1	<1	<1
DMSO	3.3	4.3	3.9	5.6
PC	7.0	6.2	6.5	8.5

2. Photoluminescence Switching of Azobenzene-Conjugated Pt^{II} Terpyridine Complexes by *trans*-to-*cis* Photoisomerization

Molecules in which emission properties can be switched by delivering photons are valuable for constructing all photon-mode molecular devices. As there are many luminescent metal

complexes, we attempted to control the photoluminescence properties by photoisomerization of the azobenzene moiety in an azobenzene-attached terpyridine complex. We employed square-planar Pt^{II} complexes, **10** and **11** (Chart 4),⁵² because the complexes containing the terpyridine ligand in solid or fluid solution are strongly luminescent in the visible region, with several emission modes due to intra-ligand π - π^* , MLCT, and inter-molecular π - π or Pt-Pt interaction.⁵³⁻⁶⁶ Although there have been some reports on fluorophores connected with azobenzenes,^{18,20,67} information on the *cis*-isomer is insufficient, probably because of its instability.

In the UV-vis absorption spectrum of **10**, the intense azo π - π^* band of ligand **1** at 350 nm is overlapped with the weak MLCT bands of the complex unit. Photoirradiation of a solution of **10** and a solution of **11** in DMF using 366-nm light causes *trans*-to-*cis* photoisomerization (Fig. 4). The *cis* form of **10** exhibits the ^1H NMR signals in a higher magnetic field com-

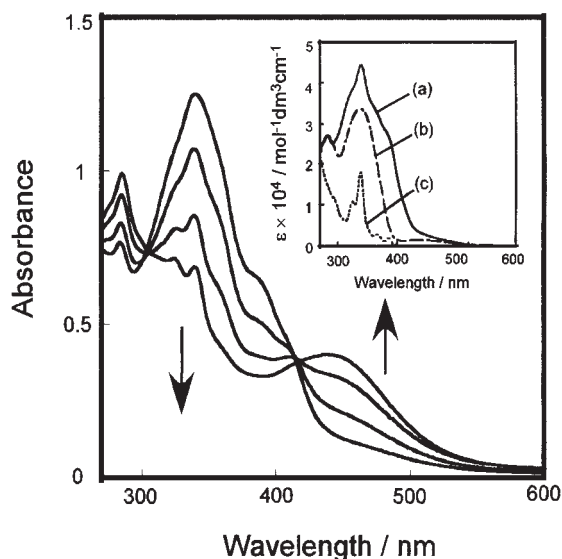


Fig. 4. UV-vis spectral change of $10 \cdot 2PF_6$ in PC (3.0×10^{-5} mol dm $^{-3}$) upon irradiation at 366 nm for 50 min. Inset: UV-vis absorption spectra of $10 \cdot 2PF_6$ (a), **1** (b), and $[Pt(py)(tpy)](PF_6)_2$ (c) (Reprinted with permission from Ref. 52).

pared to those of the *trans* form in DMF- d_7 , similar to the Rh^{III} complex as previously reported,^{33,34} and a peak of the *cis* –N=N– stretching vibration occurs at 1530 cm $^{-1}$ in the IR spectrum.^{36–38} As for both **10** and **11**, *cis*-to-*trans* isomerization occurs in DMF by both photoirradiation with visible light (wavelength > 430 nm) and by heat.

Emission spectral changes in the process of *trans*-to-*cis* isomerization were observed even for the free ligand, **1**. The emission intensity in the *cis* form is four times stronger than that of the *trans* form; the maximum excitation wavelength and emission wavelength are 300 and 500 nm, respectively. Compared with the emission spectrum of the terpyridine ligand,⁶⁸ enhanced emission is assigned to the terpyridine $^3\pi-\pi^*$ state. The emission spectral changes of **10** are more dramatic by

the *trans*-*cis* conformation change. There are four peaks at 325/480, 375/480, 300/600, and 450/600 nm in the three dimensional excitation/emission wavelength contour plot of the *cis* form, and the latter two peaks are much higher than the former two. The excitation spectrum of the emission at 600 nm for the *cis* form is identical to the UV-vis spectrum of the *cis* form. The emission lifetime was measured as 40 μ s, indicating that the emission is assignable to Pt 3MLCT , judging from the similarity in the emission behavior of Pt(py)(tpy) (τ = 8 μ s)⁵² and other Pt-terpyridine complexes previously reported.^{52–65} It should be noted that the *trans* form is totally non-luminescent at the excitation wavelength of 450 nm, as shown in Fig. 5. The absorbance of the *trans* and *cis* forms at 450 nm differs greatly; there is very weak absorption due to a forbidden azo $n-\pi^*$ transition in the *trans* form, but an intense broad absorption band appears in the *cis* form. This suggests that the interaction between azo $n-\pi^*$ and Pt MLCT at the excited states is stronger in the *cis* form than in the *trans* form. As for **11**, a similar emission spectral change was observed due to the *trans*-*cis* conformation change.

There are two significant differences in the emission properties of the Pt complexes compared with the free ligand, **1**. First, the excitation wavelength and emission wavelength are shifted to the lower energy by 150 nm. Second, the difference in emission intensity between the *trans* and *cis* forms is more significant, since the *trans* form of the complexes shows absolutely no emission. As noted above, azobenzene-conjugated Ru complexes did not undergo sufficient *trans*-to-*cis* photoisomerization, and a weak emission was present even in the *trans* form.³² Accordingly, the azobenzene-conjugated Pt complexes could be promising multifunctional materials, because *trans*-*cis* conformation change is linked with the complete off-on switching of emission.

3. Reversible *trans*-*cis* Photoisomerization of Azobenzene-Attached Bipyridine Ligands Coordinated to Cobalt Using a Single UV Light Source and the Co^{III}/Co^{II} Redox Change

As described above, the photochemical behavior of azobenzene-attached bis(terpyridine)cobalt was investigated, and re-

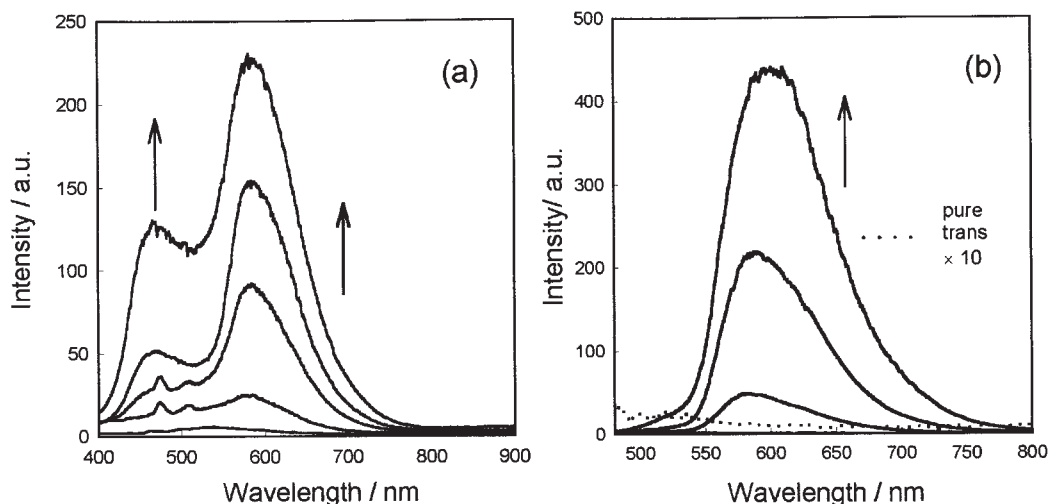
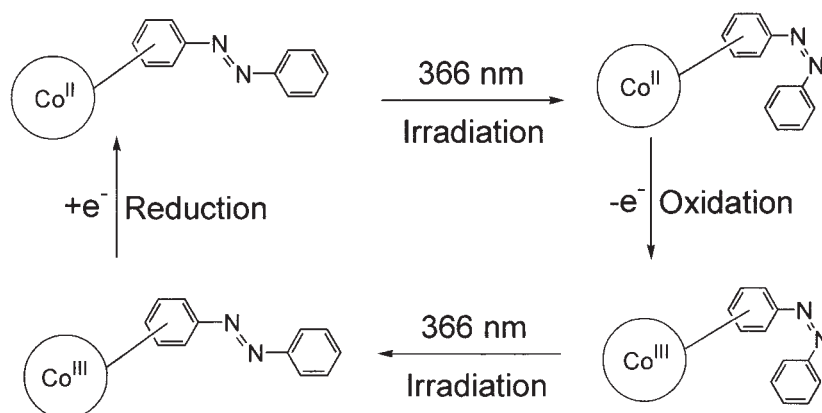


Fig. 5. Emission spectral changes of $10 \cdot 2PF_6$ in EtOH-MeOH-DMF = 5:5:1 (v/v) at 77 K upon irradiation with 366-nm light for 8 min. The excitation wavelengths were 337 nm (a) and 450 nm (b) (Reprinted with permission from Ref. 52).



Scheme 1.

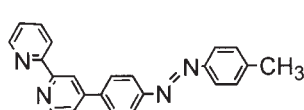
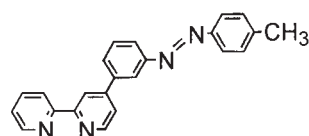
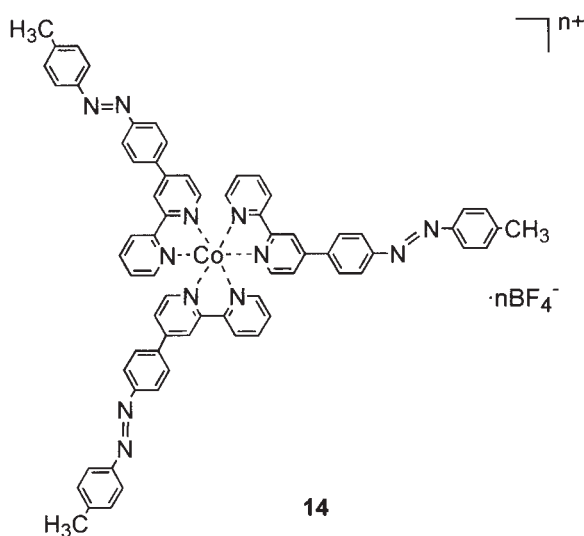
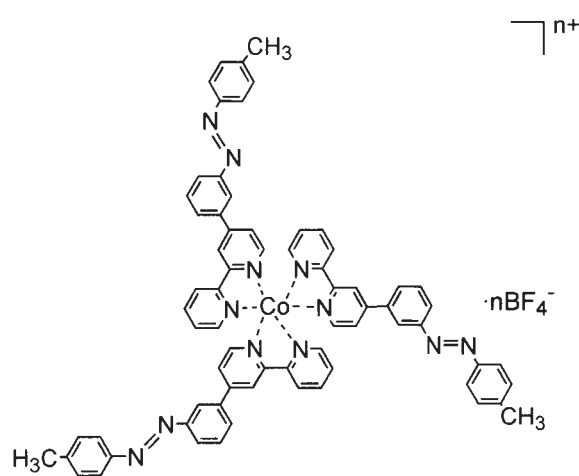
**12****13****14****15**

Chart 5.

versible *trans*–*cis* isomerization using UV and visible light in the Co^{II} state was found. We also carried out research on the azobenzene-attached tris(bipyridine)cobalt system. In this system, we watch the difference in photoisomerization by the oxidation state of the Co center, because both the Co^{II} and Co^{III} complexes are fairly stable in air under ambient conditions and their electronic interaction with the azobenzene moiety should be dissimilar. As a result of this research, the first example of reversible *trans*–*cis* isomerization of the azo group has been achieved through a combination of photoirradiation and a redox cycle between Co^{II} and Co^{III} ; this makes possible both forward and backward isomerization in response to irradiation

with a single light source (Scheme 1). Two azobenzene-attached bipyridine ligands with different conjugations between the bipyridine and azobenzene moieties, **12** and **13**, were synthesized, and their Co^{II} and Co^{III} complexes, **14** from **12** and **15** from **13**, respectively, were employed in this system (Chart 5).^{69,70}

In a cyclic voltammogram of **14**, a reversible redox wave of $\text{Co}^{\text{III}}/\text{Co}^{\text{II}}$ and a quasi-reversible one of $\text{Co}^{\text{II}}/\text{Co}^{\text{I}}$ are observed at -0.15 and -1.27 V vs Fc^+/Fc in dichloromethane, respectively. UV–vis absorption spectra of **12**, **14**· 2BF_4 , and **14**· 3BF_4 show π – π^* bands due to the azo group at $\lambda_{\text{max}} = 345$ nm ($\epsilon = 3.5 \times 10^4 \text{ mol}^{-1} \text{ dm}^3 \text{ cm}^{-1}$), 360 (1.1×10^5), and 374

(9.7×10^4), respectively. An increase in the electron-withdrawing effect on the azo group in response to the oxidation from Co^{II} to Co^{III} results in a lower energy of the $\pi\text{--}\pi^*$ band.⁷¹ Upon irradiation to the dichloromethane solution of **12** with a UV light at 366 nm, the $\pi\text{--}\pi^*$ band decreases and the $\text{n--}\pi^*$ band of the azo group at 445 nm increases in intensity, showing a typical *trans*-to-*cis* isomerization of the azobenzene moiety. The molar ratio of the *cis* form reaches 92% in the photostationary state (PSS). The spectral change of the Co^{II} complex, **14**· 2BF_4 , in dichloromethane is essentially identical to that of **12** upon irradiation with the 366-nm light, and 40% of the *trans*-azobenzene moiety is changed into the *cis* form in PSS. The irradiation with 438-nm light reverses the spectral change, indicating a *cis*-to-*trans* isomerization. Intriguingly, only a slight decrease in absorbance of the $\pi\text{--}\pi^*$ band of the Co^{III} complex, **14**· 3BF_4 , is observed under the same 366-nm light irradiation, suggesting that the *cis*-to-*trans* back reaction of the Co^{III} complex is much more effective than that of the Co^{II} complex in PSS (vide infra).

The difference in the *cis* form concentrations in PSS between Co^{II} and Co^{III} described above indicates that changing the redox state from Co^{II} to Co^{III} might make possible a reversible *trans*-*cis* conversion by single monochromatic light irradiation. The following experimental results confirm this hypothesis. The dichloromethane solution of the *trans* form of **14**· 2BF_4 was irradiated with 366-nm light to reach PSS (Fig. 6a), and the resulting mixture of *trans* and *cis* forms was oxidized with a stoichiometric amount of 1,1'-dichloroferrocenium hexafluorophosphate, $[\text{Fe}(\eta^5\text{-C}_5\text{H}_4\text{Cl})_2]\text{PF}_6$ ($E^0 = 0.19$ V vs Fc^+/Fc) (Fig. 6b).⁷² The ratio of the *cis* form remained constant after the oxidation, and the thermal isomerization to the *trans* form proceeded very slowly in the dark because the recovery of absorbance of the $\pi\text{--}\pi^*$ band was not pronounced in intensity for more than 30 min. When the oxidized solution was exposed again to 366-nm light, the *cis*-to-*trans* photoisomerization promptly occurred to create the *trans*-rich PSS that was characteristic of the Co^{III} state, accompanied by a fast increase in the absorbance of the $\pi\text{--}\pi^*$ band within a few minutes (Fig. 6c). The Co^{III} complex in PSS upon irradiation with the 366-nm light was re-reduced with a stoichiometric amount of 1,1'-acetylferrocene, $[\text{Co}(\eta^5\text{-C}_5\text{H}_4\text{COCH}_3)_2]$ ($E^0 = -0.76$ V vs Fc^+/Fc),⁷³ and the exposure to the same 366-nm light resulted in a *trans*-to-*cis* isomerization to reach a different PSS that was characteristic of the Co^{II} state. These results suggest that a reversible *trans*-*cis* isomerization can be achieved by a combination of the reversible redox change between Co^{II} and Co^{III} and irradiation with a single UV light source, which is a novel route differing from the reversible isomerization of general organic azobenzenes with a combination of $\pi\text{--}\pi^*$ and $\text{n--}\pi^*$ excitation employing both UV light and visible light, respectively (Scheme 1).

The redox-coupled photoisomerization system described above enables continuous control of total conversion to the *cis* form of azobenzene moieties in PSS by means of a continuous change in the Co^{II} to Co^{III} complex molar ratio within a range of 6–40% upon irradiation with monochromatic 366-nm light. A similar continuous control of the conversion ratio of the *cis* form for organic azobenzenes can be achieved by tuning the relative intensities of two different monochromatic light

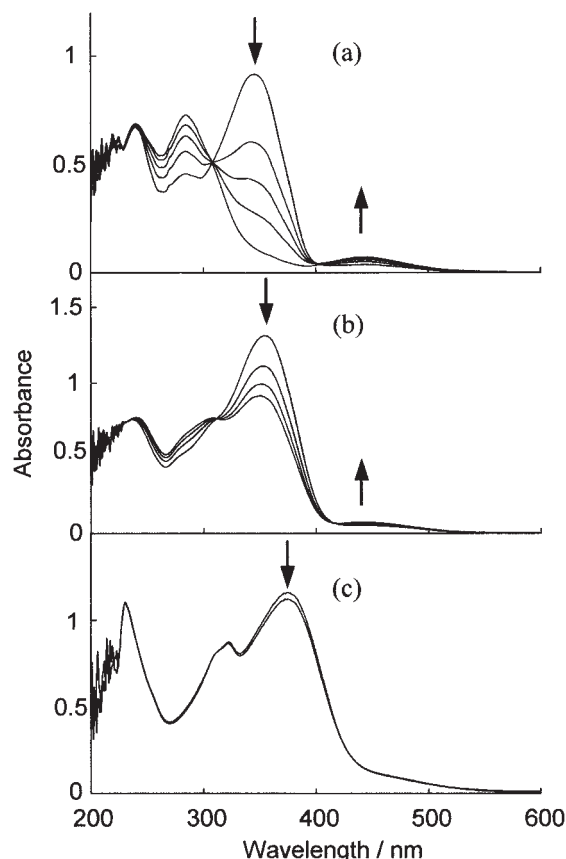


Fig. 6. UV-vis absorption spectral change of **12** (2.62×10^{-5} mol dm $^{-3}$) (a), **14**· 2BF_4 (1.17×10^{-5} mol dm $^{-3}$) (b), and **14**· 3BF_4 (1.20×10^{-5} mol dm $^{-3}$) (c), in CH_2Cl_2 upon irradiation with a 366-nm light (Reprinted with permission from Ref. 69).

sources or by selection of a suitable excitation wavelength closely associated with overlapping of the $\pi\text{--}\pi^*$ and $\text{n--}\pi^*$ bands. Compared with these photochemical methods, the combination of the photoisomerization and the redox processes of the metal complex-conjugated azobenzene is a more facile and precise pathway to adjust the *cis* conversion ratio.

A successful enlargement of the *trans*/*cis* conversion range was accomplished by using the redox reaction in the *meta*-substituted cobalt complex, **15**; an efficient reaction was induced by altering the substitution position between the bipyridine and azo moieties, thereby weakening their electronic interaction.⁷⁰ In a cyclic voltammogram of **15** in $\text{Bu}_4\text{NClO}_4\text{--MeCN}$, a reversible $\text{Co}^{\text{III}}/\text{Co}^{\text{II}}$ wave was observed at -0.11 V vs Fc^+/Fc , coincident with the *para*-analog, **14**. The UV-vis absorption spectrum of the ligand **13** shows an azo $\pi\text{--}\pi^*$ band at 327 nm, which is blue-shifted compared with that of **12** (342 nm). In **12**, the conjugation extension to the bipyridine moiety lowers the π and π^* energy gap, and causes a red shift of the $\pi\text{--}\pi^*$ absorption band. The azo $\pi\text{--}\pi^*$ band of **15**· 3BF_4 locates at a longer wavelength than that of **15**· 2BF_4 , which is a tendency similar to that of the complexes, **14**· 3BF_4 and **14**· 2BF_4 , but the difference in the former is not as large as that in the latter. This red-shift of the azo $\pi\text{--}\pi^*$ band may be caused by an electron-withdrawing effect of cobalt cation, which can be represented as $\text{Co complexes of } \mathbf{12} > \text{Co complexes of } \mathbf{13}$

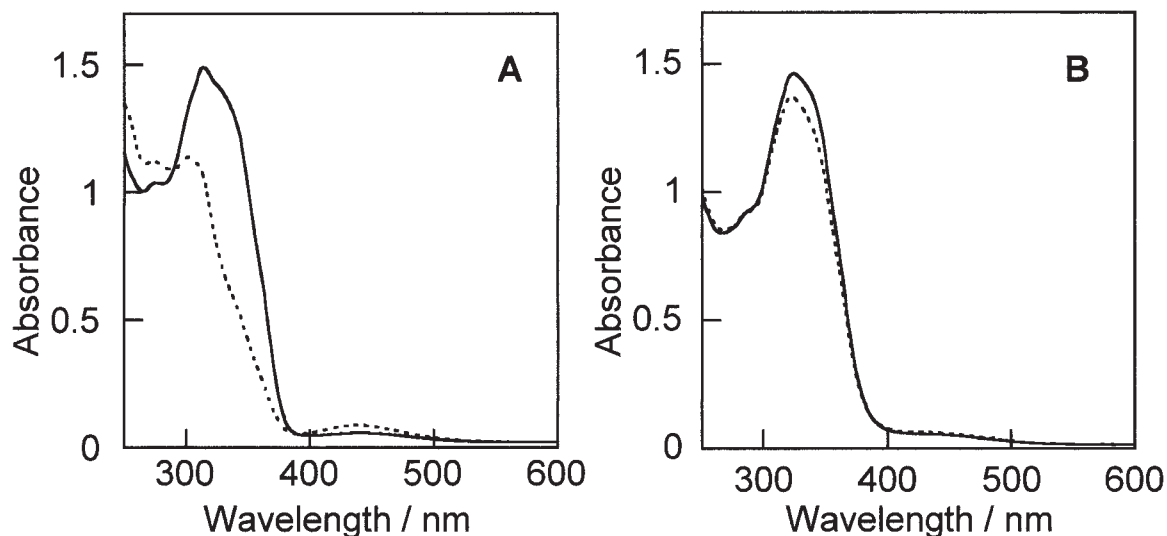


Fig. 7. Absorption spectral changes of (a) $15 \cdot 2\text{BF}_4$ ($1.53 \times 10^{-5} \text{ mol dm}^{-3}$) and (b) $15 \cdot 3\text{BF}_4$ ($1.32 \times 10^{-5} \text{ mol dm}^{-3}$) upon irradiation with monochromatic 366-nm light in CH_2Cl_2 ; at the initial state (all-*trans* form) (solid line) and at PSS (dashed line) (Reprinted with permission from Ref. 70).

and $\text{Co}^{\text{III}} > \text{Co}^{\text{II}}$.

Upon irradiation with 366 nm monochromatic light, *trans*-to-*cis* photoisomerization proceeded; the *cis* molar ratio reached 57% in PSS in $15 \cdot 2\text{BF}_4$ (Fig. 7). On the other hand, the *cis* molar ratio remained 9% at most, and also reached PSS in $15 \cdot 3\text{BF}_4$ in response to 366-nm light irradiation (Fig. 7). Thus, the difference between Co^{II} and Co^{III} is 48%, which is much improved from the 34% difference between the *para* complexes, $14 \cdot 2\text{BF}_4$ and $14 \cdot 3\text{BF}_4$.

It is clear that this enlargement of the difference between Co^{II} and Co^{III} in *meta* complexes is based on the modulation of electronic interaction between the cobalt ion and the azo moiety. In both $15 \cdot 2\text{BF}_4$ and $15 \cdot 3\text{BF}_4$, the *cis* formation efficiency (*cis* molar ratio/*trans* molar ratio) with 366-nm light was doubled compared to that of $14 \cdot 2\text{BF}_4$ and $14 \cdot 3\text{BF}_4$, and the difference between Co^{II} and Co^{III} was increased. This is because both the Co^{II} and Co^{III} cations have an effect, through π -conjugation, of suppressing the *cis* formation of the azo moiety, and this effect can be weakened by *meta* substitution. There are two possible explanations for the suppression of *cis* formation by coordination to cobalt: i) the *trans*-to-*cis* isomerization efficiency falls as the nature of the π - π^* band is transformed during coordination to a cobalt ion; and ii) the *cis*-to-*trans* back-isomerization by excitation of the *cis* isomer at 366 nm occurs in a good yield. The former explanation should be adequate, because there is a relation between the π - π^* band position of the *trans* isomer and the *cis* molar ratio formed in response to 366 nm irradiation. When the azo π - π^* band of the *trans* isomer is found in longer wavelength, the efficiency of isomerization to the *cis* isomer drops. To investigate further, we measured the *trans*-to-*cis* photoisomerization quantum yields of Co^{II} complexes. In $15 \cdot 2\text{BF}_4$, the quantum yield ($\Phi_{t \rightarrow c} = 0.11$) is almost the same as that of azobenzene^{39–47} ($\Phi_{t \rightarrow c} = 0.10$), but a lower value ($\Phi_{t \rightarrow c} = 0.07$) was obtained in $14 \cdot 2\text{BF}_4$. This result has proved that the coordination to a cobalt ion affects the azo π - π^* excitation state through electronic interaction, suppressing the *trans*-to-*cis* isomerization efficiency. The effect seems to be

more significant in the Co^{III} complexes than in the Co^{II} complexes. Actually, the azo π - π^* absorption band was found in a longer wavelength in the Co^{III} complexes than in the Co^{II} complexes, and almost no *cis* isomer was formed by π - π^* excitation in response to 366-nm irradiation in Co^{III} .

In conclusion, the reversible *trans*-*cis* isomerization has been achieved by a combination of the reversible redox reaction between Co^{II} and Co^{III} and single UV-light irradiation for azobenzene-bound tris(bipyridine)cobalt complexes. This method should provide a new design for photochemical and electrochemical hybrid molecular devices.

4. Coordination-Synchronized *trans*-*cis* Photoisomerization of Bipyridylazobenzene Driven by a $\text{Cu}^{\text{II}}/\text{Cu}^{\text{I}}$ Redox Change

In contrast to Co, which favors formation of a hexa-coordinate tris(bipyridine) complex as noted above, Cu gives a tetra-coordinate bis(bipyridine) complex. The redox reaction of this complex is accompanied by unique structural conversion of the favorite geometry from a tetra-coordinate square planar or a penta- or hexa-coordinate structure of Cu^{II} to a tetra-coordinate tetrahedral of Cu^{I} .^{74–76} Recently, several molecular systems that incorporate a copper complex unit have been developed to induce molecular motions by electrochemical signals.^{77–79} If the structural conversion causes a ligand exchange reaction, the physical property of the ligand can be changed, depending on the coordination. We applied this possibility to the construction of a molecularly synchronized system in which the *trans*-*cis* isomerization of azobenzene-attached bipyridine was controlled by its binding/release reaction to copper driven by a $\text{Cu}^{\text{II}}/\text{Cu}^{\text{I}}$ redox change. This leads to a new reversible *trans*-*cis* isomerization switching with a single light source utilizing the combination of the dynamic motion of the metal complex with that of the azobenzene ligand.⁸⁰

A 6,6'-dimethyl-substituted, azobenzene-attached bipyridine ligand **16** was designed as a new photoactive and ligand-exchangeable molecule, and its Cu^{I} and Cu^{II} complexes, $17 \cdot \text{BF}_4$

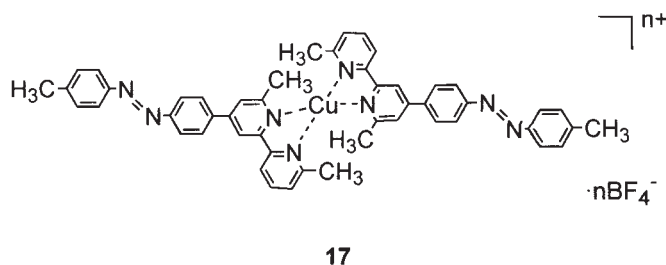
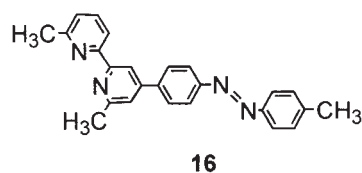


Chart 6.

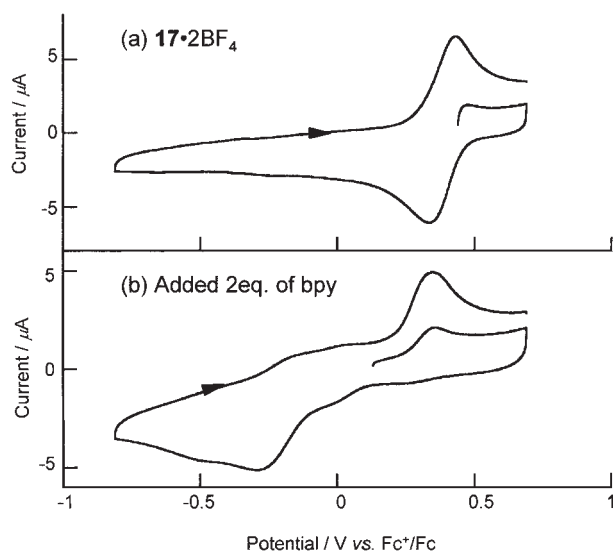


Fig. 8. Cyclic voltammograms of $17 \cdot 2\text{BF}_4$ in 0.1 mol dm^{-3} $\text{Bu}_4\text{NBF}_4\text{-CH}_2\text{Cl}_2$. (a) In pure form. (b) Mixed with 2 equivalents of bpy (Reprinted with permission from Ref. 80).

and $17 \cdot 2\text{BF}_4$, respectively, were synthesized (Chart 6). Irradiation of the ligand **16** at 365 nm causes effective *trans*-to-*cis* isomerization of the azobenzene moiety, yielding a 94% molar fraction of the *cis* isomer in PSS. On the other hand, the *cis* molar fractions at 365 nm in PSS for $17 \cdot \text{BF}_4$ and $17 \cdot 2\text{BF}_4$ were 18% and 14%, respectively. This implies that the change in the *cis* ratio in PSS by the redox change is less significant than that for the cobalt complexes **14** and **15**.^{69,70}

In a cyclic voltammogram of $17 \cdot 2\text{BF}_4$ in dichloromethane (Fig. 8a), a reversible $\text{Cu}^{\text{II}}/\text{Cu}^{\text{I}}$ redox wave is observed at 0.37 V vs Fc^+/Fc . The redox potential is considerably more positive than that of non-substituted $[\text{Cu}^{\text{I}}(\text{bpy})_2]\text{BF}_4$ ($E^{\text{O}'} = -0.12 \text{ V vs Fc}^+/\text{Fc}$), irrespective of the introduction of electron-donating methyl groups. This positive shift can be attributed to the methyl groups in **16** sterically protecting the copper center in the tetrahedral coordination structure, and preventing the formation of a favorable square-planar structure in the Cu^{II} state.⁸¹

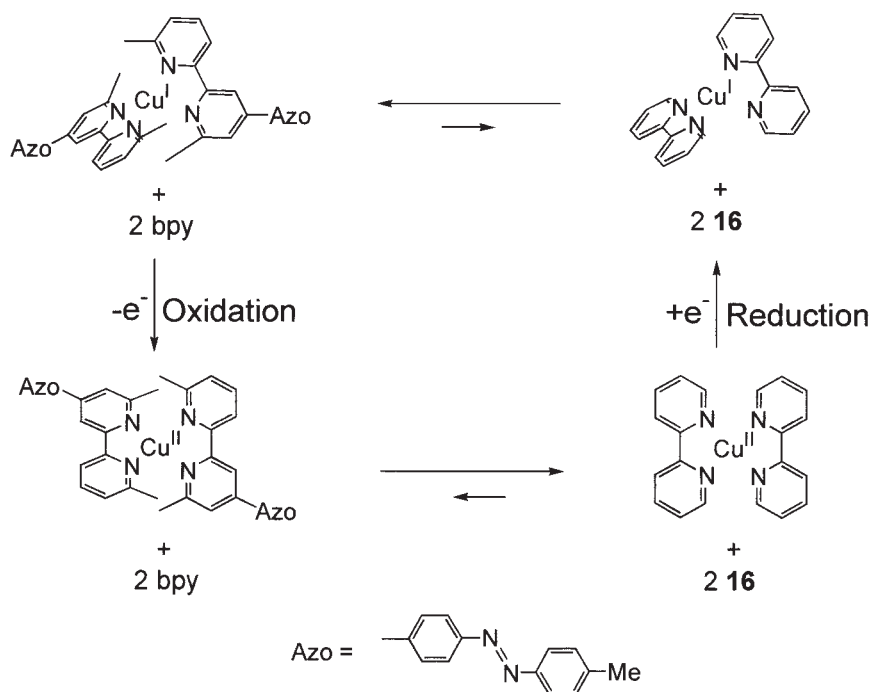
Upon addition of 2 equivalents of 2,2'-bipyridine (bpy) to the solution of $17 \cdot 2\text{BF}_4$, the oxidation wave to Cu^{II} appears at 0.32 V, similar to that without bpy, whereas the reduction wave to Cu^{I} at ca. 0.3 V disappears and a new wave is observed at -0.30 V in a cyclic voltammogram (Fig. 8b). Judging from these potentials, the major species are $17 \cdot \text{BF}_4$ and $[\text{Cu}^{\text{II}}(\text{bpy})_2]^{2+}$ at the Cu^{I} and Cu^{II} states. This indicates that a

facile ligand exchange reaction occurs on the time scale of cyclic voltammetry. This consideration was supported by the UV-vis spectral change of the complex upon addition of bpy. When bpy was added to a solution of $17 \cdot 2\text{BF}_4$, a blue shift of the azo $\pi\text{-}\pi^*$ band (352 nm) occurred in the UV-vis spectra. When 5 equivalents of bpy were added, the shift was saturated at 345 nm, identical to the $\pi\text{-}\pi^*$ band location of the free ligand, **16**. In $17 \cdot \text{BF}_4$, almost no azo $\pi\text{-}\pi^*$ band shift occurs with the addition of bpy. The driving force of this reversible ligand exchange reaction may be the difference in coordination geometry between Cu^{I} and Cu^{II} ; the Cu^{I} cation prefers the tetrahedral geometry, which the methyl groups in **16** stabilize.⁷⁶ The ligand **16** also prevents nucleophilic attacks on the copper center. On the other hand, when Cu^{I} is oxidized to Cu^{II} , the copper center prefers bpy. This is because the methyl groups in **16** cause significant steric hindrance of the coordination of the Cu^{II} cation in the favorite square-planar structure (Scheme 2).

Since the redox-controlled coordination reaction of **16** is considered to affect the electronic structure of the azo moiety, we can convert the photoisomerization behavior through a redox reaction. Thus, we investigated the photoisomerization behavior of copper complexes in the presence of bpy. When mixed with bpy, the absorption changes upon UV irradiation of the Cu^{I} and Cu^{II} complexes exhibited significant differences between these two complexes (Fig. 9). These spectra suggested that a *trans*-rich composition was achieved in the Cu^{I} sample, while a *cis*-rich composition was formed in the Cu^{II} sample in PSS, despite the use of the same UV light irradiation.

Next, the *cis* molar ratio in PSS (365 nm) vs. the amount of bpy added to the solution was examined. In the solution of $17 \cdot 2\text{BF}_4$, the *cis* molar ratio was increased with the addition of bpy, and the ratio saturated when ca. 2 equivalents of bpy were added. It is considered that the exchange reaction of the complex with bpy affords free **16**, which isomerizes efficiently to *cis* isomer. On the other hand, $17 \cdot \text{BF}_4$ shows little increase of the *cis* form with the addition of bpy, because bpy cannot displace **16** on copper. Thus, the *cis* molar ratios in PSS in $17 \cdot \text{BF}_4$ and $17 \cdot 2\text{BF}_4$, which were 18% and 14% when they were present alone, converted to 25% and 72%, respectively, when 2 equivalents of bpy were added, thereby achieving drastic changes in the isomerization behavior with altering the oxidation state of copper.

Finally, we tried to convert the oxidation state of Cu^{II} and Cu^{I} reversibly, and we did observe reversible photoisomerization with a single UV light source. Photoisomerization controlled by a reversible ligand coordination reaction was performed chemically with oxidizing and reducing agents. A mixture of $17 \cdot \text{BF}_4$ and 2 equivalents of bpy in dichloromethane was irra-



Scheme 2.

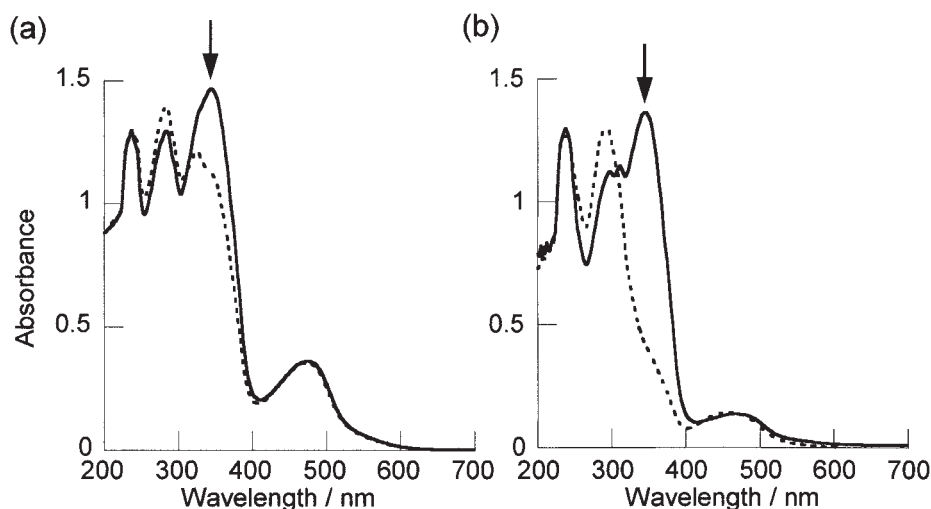


Fig. 9. UV-vis absorption spectral changes of **17**·BF₄ (2.0×10^{-5} mol dm⁻³) plus bpy (4.0×10^{-5} mol dm⁻³) (a), and **17**·2BF₄ (2.0×10^{-5} mol dm⁻³) plus bpy (4.0×10^{-5} mol dm⁻³) (b) upon photoirradiation in CH₂Cl₂. Solid and dotted lines refer to the all-*trans* form and the *trans/cis* mixture at PSS at 365 nm, respectively (Reprinted with permission from Ref. 80).

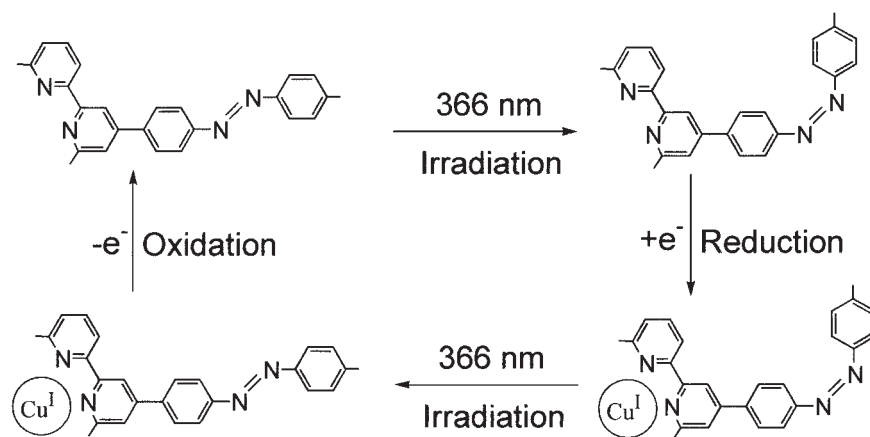
diated with 365 nm light, forming 32% of *cis* isomer. Then the same sample was oxidized to the Cu^{II} state by 1 equivalent of [Fe(η^5 -C₅H₄Cl)₂]₂PF₆ and re-irradiated with the same 365-nm light; this resulted in further *trans*–*cis* isomerization and an increase of the *cis* ratio to 70%. Then the copper was reduced to the Cu^I state with 1 equivalent of [Co(η^5 -C₅H₄COCH₃)₂] and re-irradiated with 365-nm light. The result was inverse *cis*-to-*trans* isomerization. These results demonstrate that the isomerization behavior was controllable with a single UV light source and the ligand's binding/release reaction, which is reversibly performed with the Cu^{II}/Cu^I redox change (Scheme 3).

In conclusion, the *trans*–*cis* photoisomerization behavior of the azobenzene moiety was synchronized with ligand coordina-

tion of the conjugated bpy moiety to copper. The coordination reaction can be reversibly controlled by changing the oxidation state of copper, leading to reversible *trans*–*cis* isomerization using a combination of UV light and redox reaction with a good yield of *cis* isomer.

5. Redox-Conjugated Reversible Isomerization of Ferrocenylazobenzene Using a Single Green Light Source

Azoferrocene, **18**, is one of the π -conjugated ferrocene dimers and also one of the simplest analogues of azobenzene, having two redox-active metal complex units. Its synthesis was first reported by Nesmeyanov et al. in 1961 (Chart 7).^{82,83} Although **18** has proved to be an intriguing complex since iden-



Scheme 3.

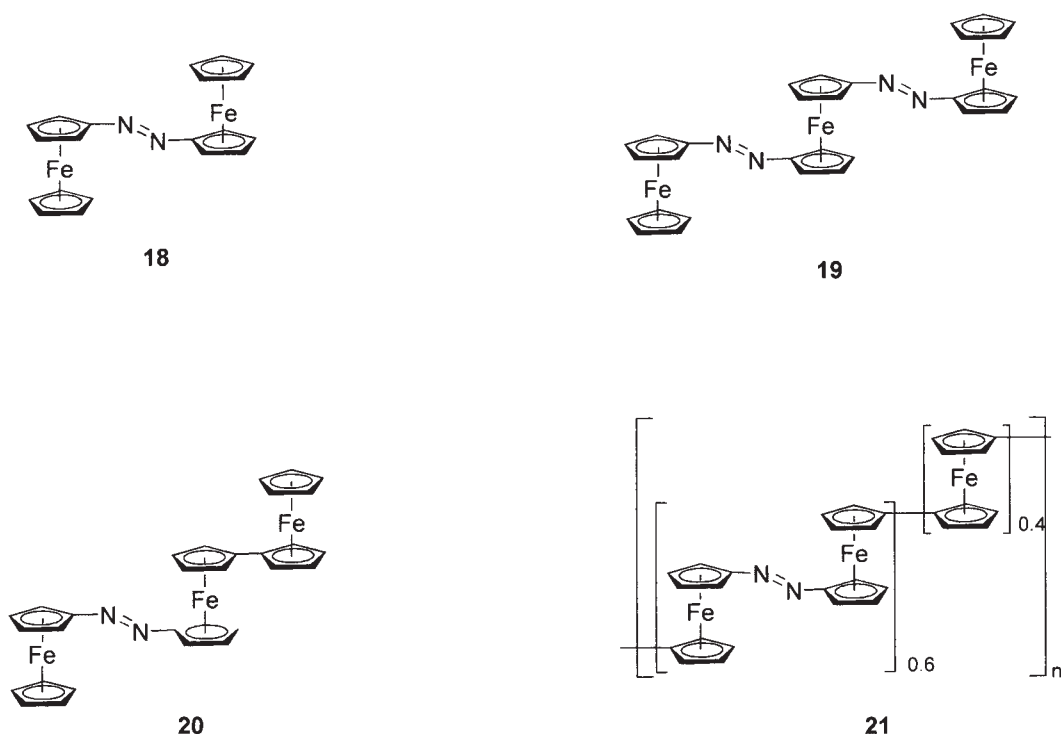


Chart 7.

tification of the azo group as the representative photoisomerizable unit, few studies have appeared on azoferrocene in more than forty years following its discovery. We carried out X-ray crystallography of an azoferrocene crystal obtained under ambient conditions; the results demonstrated that the azo moiety is in the *trans* form, and that the two cyclopentadienyl rings of the two ferrocenyl units and the azo moiety are on almost the same plane, which is ideal for π -conjugation.⁷¹ The ferrocenyl moieties are on the opposite side of the plane, and the Fe–Fe distance is 6.80 Å, indicating that there are few through-space interactions between the Fe nuclei. Higher azo-bridged ferrocene oligomers, such as trimers **19** and **20**, and a polymer, **21**, have also been prepared.⁷²

The *trans*-azo bridge is similar to the vinylene bridge in that it acts as a spacer that assists in the electron exchange between

ferrocenyl moieties. The cyclic voltammogram of **18** in $\text{Bu}_4\text{NClO}_4\text{--PhCN}$ exhibits reversible $1e^-$ oxidation waves at $E^0 = 0.08$ and 0.29 V vs Fc^+/Fc , indicating the formation of a thermodynamically stable mixed-valence cation. The mixed-valence cation of **18** formed in PhCN by $1e^-$ chemical oxidation exhibits an EPR spectrum characterized by the superposition of narrow signals ($g = 1.9$) and a broad signal ($g_{\parallel} = 3.0$, $g_{\perp} = 1.9$) due to a ferrocenium Fe^{III} cation at 7.6 K.⁸⁴ The narrow hyperfine signals in the mixed-valence cation may be due to coupling with the ring protons and the nitrogen atoms caused by the delocalization of the unpaired electronic charge over the bridging ligand, Cp--N=N--Cp ($\text{Cp} = \eta^5\text{-cyclopentadienyl}$). Similar unusual hyperfine structures were observed in the ESR spectrum of a solid sample of $[\text{Fe}_2(\text{C}_5\text{H}_4)_4]\text{I}_3$ at 77 K.⁸⁵ The trimer **19** in aprotic solvents such as CH_2Cl_2 or

THF exhibits a cyclic voltammogram showing reversible $2e^-$ and $1e^-$ oxidation waves. This behavior can be explained by the assumption that the positive charge in the monocation is localized primarily around the terminal ferrocenyl unit due to the strong electron-withdrawing effect of the azo group.^{72,86}

Azo-bridged ferrocene oligomers also show a marked dependence on the redox potentials and IT-band characteristics of the solvent, as is usual for the class II mixed valence complexes.^{87,88} A detailed analysis of the solvent effect on ν_{\max} of the IT band of the azo-bridged ferrocene oligomers **18**⁺, **20**⁺, and **20**²⁺ indicates that the ν_{\max} shift is dependent not only on the parameter in the Marcus–Hush theory, $(1/D_{\text{op}} - 1/D_s)$, where D_{op} and D_s are the solvent's optical and static dielectric constants, respectively, but also on the nature of the solvent as donor or acceptor.

In addition to the strong $\pi-\pi^*$ transition of the azo group at 318 nm, strong d- π^* transition (MLCT) bands from a Fe^{II} d-orbital to a π^* -orbital of Cp-N=N-Cp appear in the neutral *trans* form of the azo-bridged ferrocene oligomers. The absorption of the MLCT band at 534 nm diminishes, and a new band appears and increases at 672 nm with the oxidation to **18**⁺. The new band can be identified as a ligand-to-metal charge transfer (LMCT) band associated with an electron transfer from the π orbital of the azo group to a Fe^{III} d orbital. Similar LMCT bands appear in the mixed valence state of trimers **19** and **20**. A more donating solvent affords the higher IT and LMCT energies of **18–20** in the mixed-valence states, indicating a hole-transfer mechanism.⁸⁹

Photoirradiation of **18** in the *trans* form, *trans*-**18**, in MeCN exposed to UV (365 nm) light, causes a decrease of the $\pi-\pi^*$ band and an increase of a new band at 368 nm in intensity, showing isosbestic points, as displayed in Fig. 10. The photoreaction of *trans*-**18** also proceeds through MLCT with green (546 nm) light (Fig. 10).⁴⁸ This is a rare example of photoreaction using a low energy band distinct from the $\pi-\pi^*$ transition band. Photoreaction of *trans*-**18** is accelerated in polar solvents such as MeCN, PhCN, and DMSO, and greatly suppressed in less polar solvents such as toluene. This spectral change indicates the occurrence of *trans*-to-*cis* isomerization; however, the back reaction is not observed by heating or irradiation with visible light, and further study will be needed to characterize the photoproduct. Our recent study indicated that the presence of trace protons in the photoreaction media causes the irreversible photoreaction.⁹⁰

This first discovery of photoreaction by green-light irradiation exciting a low-lying MLCT (metal-to-ligand charge transfer) band for azoferrocene prompted us to seek a more stable photoisomerization molecular system. The combination of the reversible isomerization with a single light source together with the redox state change of the metal center, which was found in tris(bipyridine)cobalt complex-attached azobenzene,^{69,70} namely, “reversible isomerization using a single visible light source,” (Scheme 4), is of great interest for the following reasons. The redox-conjugated reversible isomerization cycle using a single light eliminates the need for a double-light source optical system emitting lights of different wavelength, and the utilization of green light instead of UV light is advantageous in avoiding degradation of the aromatic framework of the photo-functional molecules.

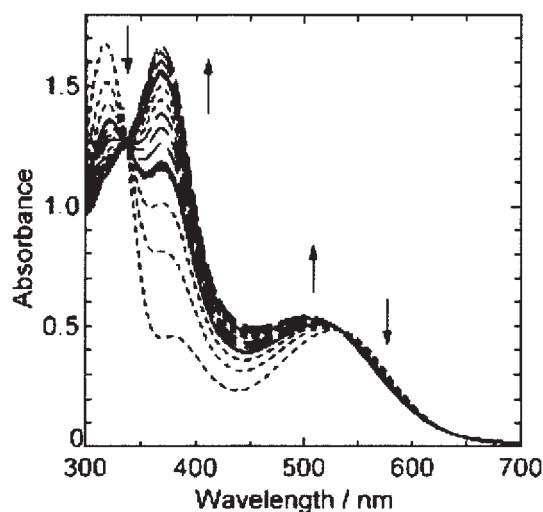
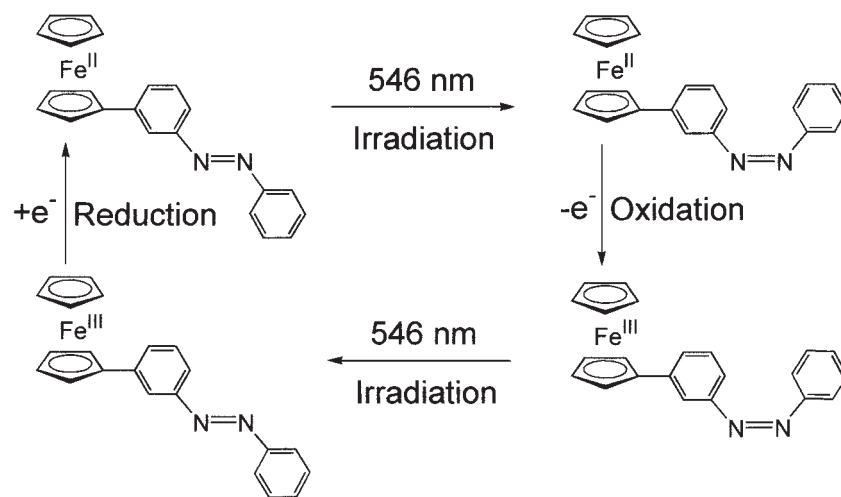


Fig. 10. UV-vis absorption spectral change of *trans*-**18** ($1.26 \times 10^{-4} \text{ mol dm}^{-3}$) in MeCN upon photo-irradiation with three bright lines ($\lambda_{\max} = 365, 436,$ and 546 nm) from a super high pressure Hg lamp. The spectra are depicted at 10-min intervals of the photo-irradiation. The irradiation with each bright line was continued for 30 min in the order of 365 (dotted lines), 436 (solid lines), and 546 (broken lines) nm, respectively (Reprinted with permission from Ref. 84).

A possible candidate for the isomerization using MLCT is the azo-ferrocene combined species. In this study, we therefore employed ferrocenylazobenzenes (Chart 8),⁹¹ one of which, 3-ferrocenylazobenzene, **22**, achieves the reversible isomerization using a single green light source by combination with the reversible redox reaction between Fe^{II} and Fe^{III} (Scheme 4).

trans-**22** shows an azo $\pi-\pi^*$ band at $\lambda_{\max} = 318 \text{ nm}$ and a weak visible band at 444 nm. The azo $\pi-\pi^*$ band decreased in intensity through green (546 nm) and UV light (320 nm) irradiation, whose wavelengths correspond to an edge of the visible band and the maximum in the azo $\pi-\pi^*$ band, respectively (Fig. 11A). ^1H NMR signals of the aromatic ring protons of the azobenzene moiety were significantly shifted to higher field positions after the light irradiation.³⁵ These spectroscopic behaviors are characteristic of the *trans*-to-*cis* isomerization. The *cis* molar ratio reached 35% in PSS upon the green-light irradiation, and the PSS was changed into a more *cis*-rich state (61% *cis* molar ratio) upon the UV light irradiation (Fig. 11A and Table 3). The quantum yield for the *trans*-to-*cis* isomerization, $\Phi_{t \rightarrow c}$, of **22** was estimated to be 0.51 for the green light (546 nm),⁴⁷ which is much higher than that (0.021) for the UV light (320 nm) and exceeds that of azobenzene ($\Phi_{t \rightarrow c} = 0.12$ (313-nm excitation)).⁴⁴ The thermal *cis*-to-*trans* isomerization of **24** was very slow and the rate constant ($k = 1.3 \times 10^{-4} \text{ s}^{-1}$ at 70°C) was consistent with that of azobenzene ($k = 1.3 \times 10^{-4} \text{ s}^{-1}$ at 70°C).

Both the chemical oxidation with $[\text{Fe}(\eta^5\text{-C}_5\text{H}_4\text{Cl})_2]\text{PF}_6$ ⁷² and the electrochemical oxidation of *trans*-**22** from Fe^{II} to Fe^{III} caused a shift of the $\pi-\pi^*$ band to higher-energy from $\lambda_{\max} = 318$ to 312 nm , then a weak LMCT band appeared at 730 nm . The reversibility of the electrochemical redox reaction between Fe^{II} and Fe^{III} was high, according to the completely reversible



Scheme 4.

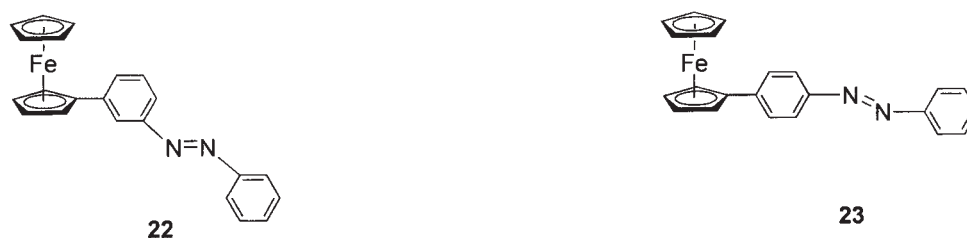


Chart 8.

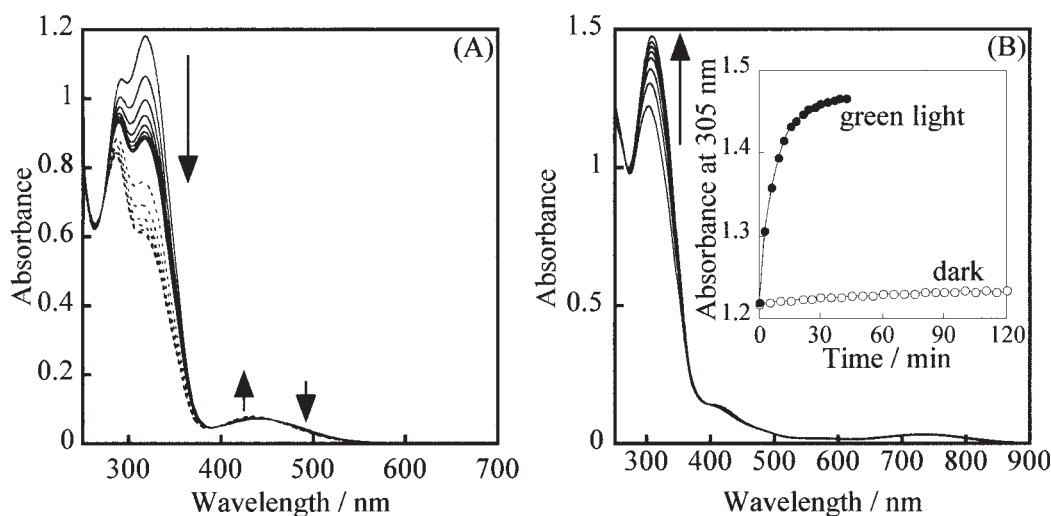


Fig. 11. (A) UV-visible absorption spectral change of *trans*-**22** (5.52×10^{-5} mol dm $^{-3}$) in MeCN upon irradiation with a monochromatic light at 546 nm for 21 min (solid lines) and subsequent irradiation at 320 nm for 4 min (dotted lines). (B) UV-visible absorption spectral change of the following sample solution upon irradiation with a monochromatic light at 546 nm; (inset) time course change in absorbance at 305 nm of the sample solution upon irradiation with a monochromatic light at 546 nm (solid circles) or in the dark (open circles). The sample solution was prepared by irradiation with a monochromatic light at 546 nm to *trans*-**22** in MeCN (5.62×10^{-5} mol dm $^{-3}$) to reach PSS and then oxidation with 1 equivalent of $[\text{Fe}(\eta^5\text{-C}_5\text{H}_4\text{Cl})_2]\text{PF}_6$ (Reprinted with permission from Ref. 91).

spectral change. Photoisomerization of the *trans*-Fe^{III} state was highly dependent on the irradiation wavelength. The decrease in absorbance of the π - π^* band in the Fe^{III} state observed under UV-light irradiation was almost entirely absent under the green-light irradiation. The large difference in the *cis* molar ra-

tios in PSS between the Fe^{II} and Fe^{III} states suggests the possibility that single green-light irradiation might induce reversible *trans*-*cis* conversion by changing the oxidation state of the iron center. The following experiments confirmed that this was the case.

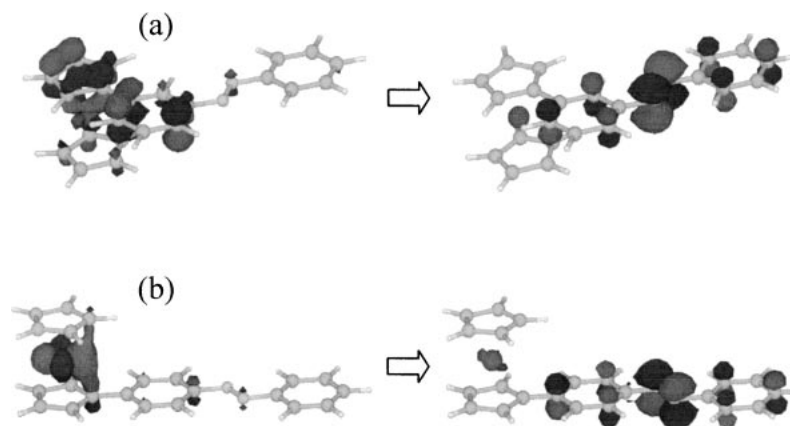


Fig. 12. The molecular orbitals contributing to the MLCT of *trans*-**22** (a) and *trans*-**23** (b) (Reprinted with permission from Ref. 91).

Table 3. *cis* Molar Ratios at the Photostationary State (PSS) of Ferrocenylazobenzenes

	Excitation wavelength/nm					
	320	350	436	500	546	600
22	61%		17%	36%	35%	
23		41%	6%	7%	6%	0%

An MeCN solution of *trans*-**22** of Fe^{II} was irradiated with green light to reach PSS (35% *cis* molar ratio), and the resulting mixture of *trans* and *cis* forms was oxidized to the Fe^{III} state immediately after addition of a stoichiometric amount of [Fe(η^5 -C₅H₄Cl)₂]₂PF₆. After the oxidation, the recovery of absorbance of the π - π^* band was not pronounced in intensity over several hours in the dark at room temperature, and the thermal isomerization to the *trans* form proceeded very slowly in the Fe^{III} state ($k = 8.7 \times 10^{-4} \text{ s}^{-1}$ at 70 °C) (Fig. 11B, inset). The green-light irradiation promoted the increase in the absorbance to reach the *trans*-rich PSS characteristic of the Fe^{III} state, suggesting that almost all of the *trans* form was photo-recovered (Fig. 12B). These results indicate that reversible *trans*-*cis* isomerization can be achieved by a combination of “on-off switching” of the MLCT character due to the redox change between Fe^{II} and Fe^{III} and single green-light irradiation. The LMCT band that appeared in the Fe^{III} state is not associated with the isomerization.

It should be noted that the photoisomerization behavior and thermal isomerization behavior of ferrocenylazobenzenes are strongly influenced by the substitution position of the ferrocenyl moiety on the benzene ring. *trans*-4-ferrocenylazobenzene (*trans*-**23**) exhibits an intense visible MLCT band (494 nm) and a largely red-shifted azo π - π^* band ($\lambda_{\text{max}} = 352 \text{ nm}$) compared to azobenzene (317 nm) or *trans*-**22** (318 nm). The *trans*-to-*cis* isomerization proceeded with $\Phi_{\text{t} \rightarrow \text{c}} = 0.0033$ by irradiation with UV light (350 nm) to reach a 41% *cis* molar ratio in PSS. However the MLCT in **23** is not effective for the *trans*-to-*cis* conversion (Table 3), whereas the *cis*-to-*trans* back reaction can be promoted even by orange light at 600 nm, which corresponds to the edge of the MLCT band, instead of blue light (~450 nm). The thermodynamic stability of the *cis* form was remarkably reduced by the oxidation, since the fast recovery of the intensity of the π - π^* band due to the transfor-

mation of the *cis* form into the *trans* form was observed immediately after the oxidation of the photo-generated *trans*-*cis* mixture at room temperature. The *cis*-to-*trans* thermal isomerization rate could be estimated as $3.8 \times 10^3 \text{ s}^{-1}$ only at a low temperature (5 °C).

It is of great interest that the green light caused a much higher *cis* molar ratio in **22** than in **25** and azobenzene. We therefore carried out time-dependent density functional theory (TD-DFT) calculations for **22** and **23** in the *trans* form, in order to determine the singlet excited state in which the isomerization occurs. The calculated excitation energies in the *trans* forms were in reasonable agreement with the experimental values, and the observed trends in the experimental absorption spectra were correctly reproduced (Table 4). Noticeable features in the nature of the excited states of the *trans*-**22** are that the azo n - π^* strongly mixes with the MLCT configuration, and that the initial orbital for the 3.02 eV MLCT state is delocalized over Fe and the Cp ring rather than localized on the iron (Fig. 12a). The presence of the MLCT character is the reason that the molar extinction coefficient of the visible band ($\lambda_{\text{max}} = 444 \text{ nm}$, $\epsilon = 1.86 \times 10^3 \text{ mol}^{-1} \text{ dm}^3 \text{ cm}^{-1}$) is much larger than that of the n - π^* band of *trans*-azobenzene ($\lambda_{\text{max}} = 444 \text{ nm}$, $\epsilon = 5.15 \times 10^2 \text{ mol}^{-1} \text{ dm}^3 \text{ cm}^{-1}$). The origin of the visible band in **22** is different from that of **23**, because the initial orbital for the 2.51 eV MLCT state of the latter is localized on the iron (Fig. 12b). The green-light-induced *trans*-to-*cis* isomerization of **22** may occur on the potential energy surface for the MLCT excited state. In fact, the almost complete absence of a response to the green light for the *cis* formation in the Fe^{III} state is caused by the disappearance of the MLCT character in the Fe^{II} state by the oxidation to Fe^{III}.

6. Synthesis of Azo-Conjugated Metalladithiolenes and Their Photo- and Proton-Responsive Isomerization Reactions

Metalladithiolenes^{92,93} with aromatic nature exhibit a number of interesting properties, including reversible redox activity^{94,95} and various chemical reactivities.^{96,97} Thus, the combination of dithiolene complexes with the azo group can afford photo-responsive multifunctional molecules. We synthesized a precursor for a new azo-conjugated benzenedithiolato ligand, **24**, as well as its Ni, Pd, and Pt complexes, **25**–**27** (Chart 9), and found reversible photoisomerization and protonation behavior;

Table 4. Experimental and Theoretical Excitation Energies to the Lowest Excited State among Those of a Similar Character

Excitation energy/eV		Oscillator strength	Assignment (Coefficient)
Expt.	Theor.		
<i>trans</i> - 22			
—	2.43	0.001	Azo n- π^* (0.55) + ML(azo π^*)CT (-0.33)
2.79	3.02	0.060	ML(azo π^*)CT (0.65)
3.90	3.49	0.693	Azo π - π^* (0.59)
<i>cis</i> - 22			
—	2.45	0.047	Azo n- π^* (0.56) + ML(azo π^*)CT (-0.21)
—	3.16	0.001	ML(azo π^*)CT (0.35) + Cp-azo π^* (0.31)
—	3.96	0.103	Azo π - π^* (0.58)
<i>trans</i> - 23			
—	2.42	<0.001	Azo n- π^* (0.66)
2.51	2.63	0.113	ML(azo π^*)CT (0.57)
3.52	3.03	0.752	Azo π - π^* (0.55)
<i>trans</i> -azobenzene			
2.79	2.42	<0.001	Azo n- π^* (0.62)
3.91	3.54	0.079	Azo π - π^* (0.56)

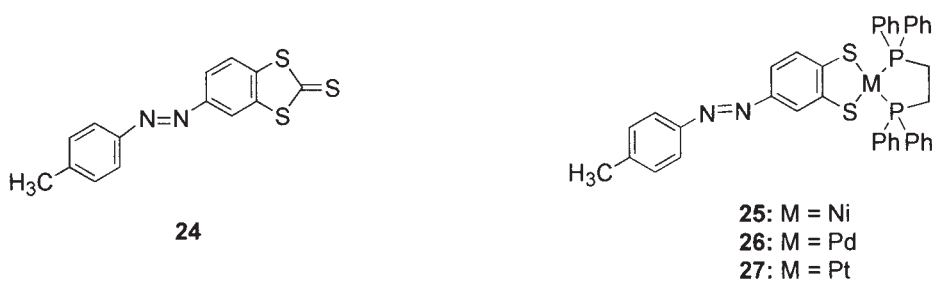


Chart 9.

besides, the protonation-catalyzed *cis*-to-*trans* isomerization of the complexes.^{98,99}

Single crystal X-ray crystallographic analyses were carried out for **25**–**27**. An ORTEP diagram of the molecular structure of **27** is displayed in Fig. 13.^{98,99} The configuration around the Pt center is a typical tetra-coordinated square-planar structure. The bond lengths of Pt–S1 and Pt–S2 are 2.310 Å and 2.316 Å, respectively, both of which lengths lie within the usual range of Pt–S distances for Pt dithiolene complexes.^{100,101} The configuration of the azo moiety is *trans*, but the planarity of the azobenzene moiety⁶⁹ is significantly distorted, with the torsion angle of C12–C7–C5–C4 being 55.3°. The bond length of N1–N2 is 1.32(2) Å, which is significantly longer than the usual 1.23–1.24 Å values for azobenzene compounds,^{12,102,103} and closer to the single bond length of charge-distributed triazene (–N[–]–N⁺=N–),^{104,105} rather than to that of a typical double bond. These novel features indicate the existence of strong conjugation between the azo and the metalladithiolene moieties.

The complexes **25**–**27** show a reduction wave ascribable to the metalladithiolene moiety, in addition to irreversible two-

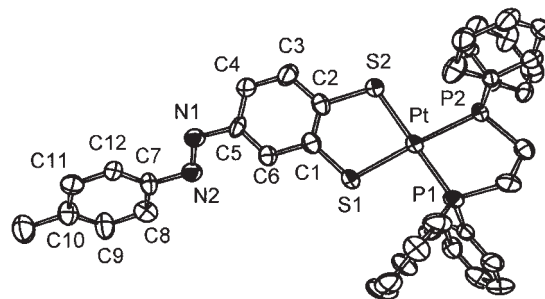


Fig. 13. ORTEP plot of **27** with 50% probability ellipsoids. Selected bond lengths [Å], angles [°] and torsion angles [°]: Pt–S1 2.310(10), Pt–S2 2.316(6), Pt–P1 2.259(6), Pt–P2 2.260(9), N1–N2 1.32(2), N1–C5 1.42(2), N2–C7 1.44(2), S1–Pt–S2 88.5(5), S1–Pt–P1 92.4(5), P1–Pt–P2 85.3(5), C4–C5–N1 116.8(17), C5–N1–N2 113.7(15), N1–N2–C7–C12 –27.7(29), C5–N1–N2–C7 174.5(16), N2–N1–C5–C6 –26.6(25) (Reprinted with permission from Ref. 98).

Table 5. Reduction and Oxidation Potentials^{a)} of **25**–**27**

Complex	$E^{0'}$, $E_{p,c}$ or $E_{p,a}$ /V vs Fc^+/Fc				
	Metalladithiolene	Azo		Metalladithiolene	Azonium ^{b)}
25	−1.93 (rev)	−1.85	−1.98	0.31	−0.29
26	−2.25 (2e [−])	−1.96	−2.08	0.38	−0.34
27	−2.60 (2e [−])	−1.95	−2.22	0.45	−0.35

a) $E^{0'}$ ($= (E_{p,c} + E_{p,a})/2$) values are denoted for reversible reactions (rev is given inside the parentheses), and $E_{p,c}$ and $E_{p,a}$ values are given for irreversible reduction and oxidation. The reduction is a 1e[−] process unless 2e[−] is specified in the parentheses. b) Potentials of new reduction wave upon addition of acid.

step 1e[−] reduction waves of the azo moiety at −1.8 to −2.2 V vs Fc^+/Fc , respectively (see Table 5). The Ni complex, **25**, shows a reversible wave at −1.93 V, which can be attributed to a Ni^{II}/Ni^I 1e[−] reduction. Compounds **26** and **27** undergo an irreversible one-step 2e[−] reduction on the metal center at −2.25 and −2.60 V, respectively. The potential and reversibility of the reduction of the metalladithiolene moieties are similar to those of the related complexes,^{106,107} and the reduction potential was found to be more negative, i.e., in the order of **27** > **26** > **25**. The reduction potentials of the azo moiety in **25**–**27** were more negative than that of azotoluene (−1.70 V vs Fc^+/Fc). This potential shift can be attributed to the strong electron donation from the metalladithiolene moiety. The donation effect was more efficient, i.e., in the order of **27** > **26** > **25**. In the oxidation of the metalladithiolene moiety, all complexes revealed a one-step irreversible wave at 0.3–0.5 V vs Fc^+/Fc . The order of these potentials was identical to that of the reduction potential. The results of these electrochemical measurements indicate that the significance of both the π electron delocalization and the π donation ability of the metalladithiolene moiety is highest in the Pt complex, **27**.

Compounds **25**–**27** exhibit an unusual proton response together with a drastic change in color, i.e., from yellow to deep green in the Ni complex, **25**; and from yellow to deep blue in the Pd and Pt complexes, **26** and **27**. Figure 14 shows the spectral changes in **25**–**27** upon addition of CF₃SO₃H in MeCN. With an increase in the amount of acid, the π – π^* transition band of the azo moiety decreased in intensity, and a new strong band appeared in the visible region. Reverse spectral changes were achieved with the addition of potassium *t*-butoxide. This spectral behavior was similar to that of the *N*-heterocycle-substituted metalladithiolenes,^{108–110} indicating that protonation of the azo moiety had taken place (Scheme 5). The single protonation is supported by the results of ESI-mass spectroscopic measurements. Upon the addition of acid, the reduction wave of the azo moiety disappeared, and a new reduction wave was observed at a more positive potential (−0.29 to −0.35 V vs Fc^+/Fc). This finding clearly demonstrates that the protonation of the azo moiety induces a significantly positive shift of the azo reduction potential. The reduction potentials of the protonated azo moiety were in the order **27** > **26** > **25**, indicating the order of stability of the protonated azo moiety. It can be deduced from these results that the protonated azo moiety is stabilized by the π electron donation from the dithiolene ring, which is the most efficient in the Pt complex, **27**.

Figure 15 shows UV–vis absorption spectra of **25**–**27** in MeCN before and after photoirradiation with UV light at 405

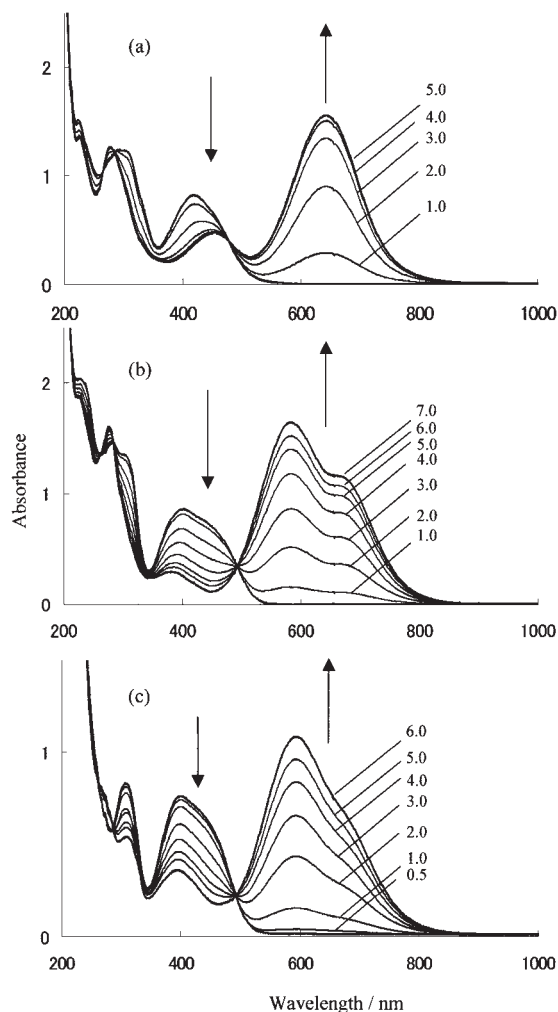
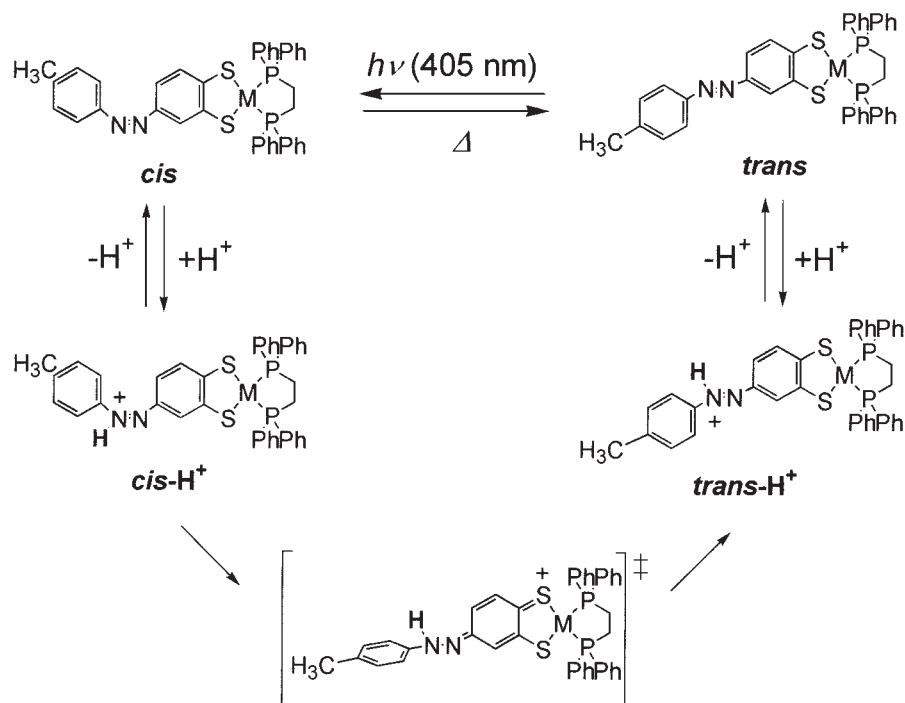


Fig. 14. UV–vis spectral changes of **25** (a), **26** (b), and **27** (c) upon addition of CF₃SO₃H in MeCN. The numbers in the figure refer to the mole equivalents of the acid to the complexes (Reprinted with permission from Ref. 99).

nm. The π – π^* transition bands ascribable to the azo moiety in the *trans* form appear at $\lambda_{\max} = 405$ nm ($\epsilon_{\max} = 1.82 \times 10^4$ mol^{−1} dm³ cm^{−1}), 405 nm (2.23×10^4 mol^{−1} dm³ cm^{−1}), and 405 nm (2.37×10^4 mol^{−1} dm³ cm^{−1}) for **25**, **26**, and **27**, respectively. These bands are significantly shifted to a lower energy compared with those of regular azobenzene derivatives,¹¹ an effect which was due to strong conjugation and high delocalization between the metalladithiolene and the azo moi-



ety. In regular organic azobenzenes, a nearly linear correlation exists between the lower energy shift of the π - π^* transition band and the stability of the *cis* form,^{111–113} and thus some of these compounds with a lower shifted π - π^* transition band may not have shown any efficient photo-response.¹¹ Despite the large low-energy shift of the π - π^* transition, **25–27** showed a distinguishable reversible photo-response. The π - π^* transition band decreased in intensity after photoirradiation, indicating the occurrence of *trans*-to-*cis* photoisomerization. The *cis*-to-*trans* reverse reaction occurred, allowing perfect recovery of the spectra of the *trans* forms, in response to photoirradiation at 360 nm in **25**, and at 310 nm in **26** and **27**, respectively. The reversible isomerization reaction was also observed by ¹H NMR spectroscopic measurements. The integration ratio of the signals for the *trans* and *cis* forms indicated that ca. 40% of the *trans* form was converted to the *cis* form by photoirradiation at 405 nm in PSS. Although the transitions corresponding to these UV-light energies have not been specified, it is intriguing that the *cis*-to-*trans* isomerization is promoted by UV light with an energy higher than the π - π^* transition, since the regular azobenzenes undergo isomerization by irradiating the n - π^* band in the visible region.¹¹⁴

The proton response of the *cis* form was then investigated. When a slight amount of acid was added to a solution containing *cis*-**25–27** prepared by photoirradiation, immediate *cis*-to-*trans* transformations were observed. The rate constants of *cis*-to-*trans* thermal and proton-catalyzed isomerization upon addition of 0.01 equivalents of CF₃SO₃H for **25–27** at 23.3 °C are displayed in correlation with the reduction potentials of the metalladithiolenes moiety in non-protonated forms in Fig. 16. The rate constant of thermal isomerization, k (s⁻¹), was independent of the differences among the central metals, whereas the rate constant of proton-catalyzed isomerization, k_{acid} (s⁻¹), strongly depended on the metal center. The k_{acid}

reaches to 2×10^{-6} s⁻¹, which is 200 times larger than k , in the Pt complex **29**, whereas no significant acceleration by addition of the acid under the same conditions was observed for azobenzene ($k = 2 \times 10^{-6}$ s⁻¹, $k_{\text{acid}} = 3 \times 10^{-6}$ s⁻¹). A positive correlation existed between the rate constant, k_{acid} , and the reduction potential of the metalladithiolenes. This result indicates that the rate constants of the proton-catalyzed isomerization are exponentially proportional to the redox potentials of the metalladithiolenes, and that the acceleration is rendered efficient by shifting the reduction potential in the negative direction. It can be deduced that the reduction potential of the metal center is closely related to the electron withdrawing ability of the metal center, which accompanies the electron donation ability of the dithiolenes ring. In the case of the Pt complex **27**, the reduction potential of which was more negative than that of **25** and **26**, strong donation to the azo group was exhibited; such donation stabilized the transient state with the resonance effects. Accordingly, the acceleration of isomerization was closely related to the reduction potential of the metal center.

The proton-assisted phenomenon indicated that a protonated *cis* form, *cis*-H⁺, instantly produced the *trans* form, *trans*-H⁺, followed by the formation of the *trans* form accompanying deprotonation (Scheme 5). In this isomerization, it can be presumed that the transient structure was the charge-distributed structure, in which the protonated nitrogen atom changed its hybridization from sp² to sp³. This activated species, with a substantial single-bond character in the azo group, was stabilized by the strong conjugation between metalladithiolenes and the azo moiety, and thus the rotational barrier for the *cis*-to-*trans* isomerization was expected to be much smaller than that expected for the thermal isomerization. The reduction in activation energy caused acceleration in the rate of the *cis*-to-*trans* isomerization. In conclusion, azo-conjugated metalladithiolenes exhibited a novel isomerization behavior, i.e., “pro-

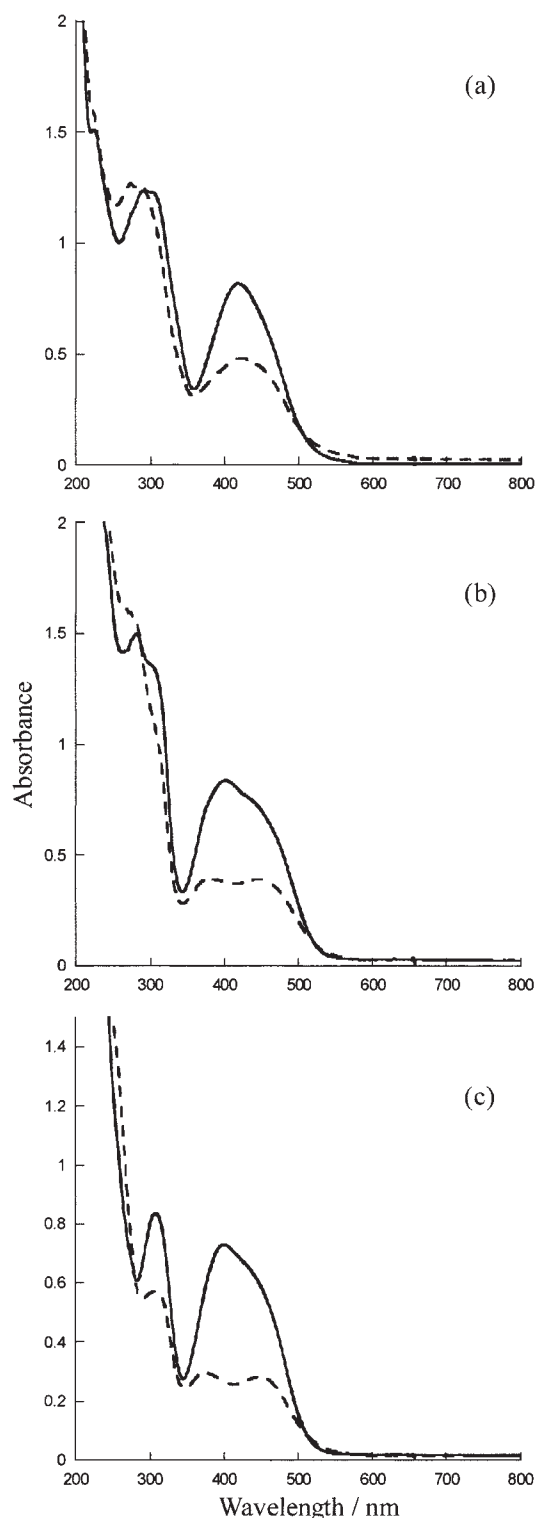


Fig. 15. UV-vis spectra of **25** (a), **26** (b), and **27** (c) in MeCN before (solid line) and after (dotted line) photoirradiation by UV light at 405 nm (Reprinted with permission from Ref. 99).

ton-catalyzed *cis*-to-*trans* isomerization". Based on the mechanism of the proton-catalyzed *cis*-to-*trans* isomerization, it can be predicted that the π donation ability of the dithiolene ring may have a considerable influence on the isomerization behav-

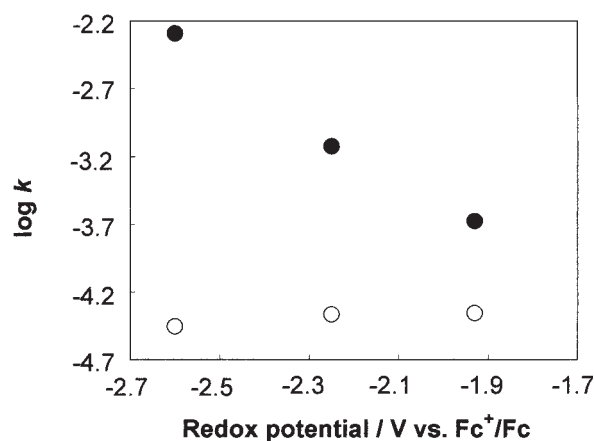


Fig. 16. Correlation between redox potentials and rate constant k (white) and k_{acid} (black) for **25–27** (Reprinted with permission from Ref. 99).

ior. The type of central metal had a dominant effect on the electronic state of the dithiolene ring; isomerization could thus be controlled in such instances by use of different metal centers.



The results described above indicate that the azo-conjugated metalladithiolene system shows *trans*-*cis* isomerization behavior responsive to both photons and protons, and would thus be useful for the development of a multi-mode switching and information storage system at the molecular level.

7. Concluding Remarks

We here described six different systems comprising azo and transition metal complex moieties. They show unique behaviors that have not been seen in common organic azo compounds. Examples of such behaviors and their relation to the original properties of azo and transition metal complex moieties are summarized in Table 6. For the realization of such behaviors by accumulation of the original properties of the azo and complex moieties, appropriate electronic and steric interactions between them are important. No multi-functionality appears when the interaction is too weak, and their original functions are too much perturbed when the interaction is too strong. It is interesting that MLCT transition in Ru and Fe terpyridine complexes works to prevent photoisomerization by absorbing the energy, whereas excitation of only the MLCT band causes the isomerization in ferrocenylazobenzenes. This should be due to the difference in nature of the π^* orbital, which localizes around the terpyridine moiety in the former but delocalizes over the azo moiety in the latter. The approach used here to create new types of photochromic materials with multi-mode functions via properly designed azo-conjugated metal complexes might be applicable to the combination of other metal complexes and other photochromic molecules.

The author thanks the following people who worked on the present study: co-workers at the University of Tokyo are Dr. Masato Kurihara, Dr. Kenya Kubo, Masaru Kurosawa, Dr. Tomona Yutaka, Dr. Masayuki Nihei, Shoko Kume, Takayuki Matsuda, Akira Hirooka, Ichiro Mori, Dr. Takuya Nankawa, and Dr. Jun Mizutani; and collaborators are Prof. Naoto Tamai and K. Matsumura at Kwansei Gakuin University, Prof.

Table 6. Relation of the Properties of Metal Complex and Azo Moieties for Manifesting Novel Properties of Azo-Conjugated Metal Complexes

Properties of the metal complex moiety	Examples of the metal complex moiety	Properties of the azo-conjugated metal complex	Properties of the azo moiety
Redox reaction	$[\text{Co}(\text{bpy})_3]^{3+/2+}$	Single light photoisomerization with redox change	
Ligand exchange	$[\text{Cu}(\text{bpy})_3]^{2+/+}$		
	$[\text{FeCp}_2]^{+/0}$	MLCT photoisomerization	
MLCT absorption	$[\text{Fe}(\text{tpy})_2]^{2+}, [\text{Ru}(\text{tpy})_2]^{2+}$	Quenching of photoisomerization	
Photoluminescence	$[\text{PtCl}(\text{tpy})]$	Switching of photoluminescence by photoisomerization	
Ionic structure	$[\text{Rh}(\text{tpy})_2]^{3+}$	Strong effect of counterion and solvent on the photoisomerization	
Bulkiness		Irreversible photoisomerization	
Electron donation	$[\text{M}(\text{dppe})(\text{S}_2\text{C}_6\text{H}_3\text{R})]$ (M = Ni, Pd, Pt)	Proton-catalyzed photoisomerization	Thermal isomerization
			Protonation

Manabu Sugimoto at Kumamoto University, Prof. Masahiro Irie and Prof. Takeshi Kawai at Kyushu University, and Dr. S. Furusho at Jasco International, Co., Ltd. This work was supported partly by Grants-in-Aid from the Ministry of Education, Culture, Sports, Science and Technology, and The 21st Century COE Program for Frontiers in Fundamental Chemistry.

References

- C. Joachim, J. K. Gimzewski, and A. Aviram, *Nature*, **408**, 541 (2000).
- H. Nishihara, M. Kurashina, and M. Murata, *Macromol. Symp.*, **196**, 27 (2003), and references cited therein.
- M. Kurashina, M. Murata, T. Watanabe, and H. Nishihara, *J. Am. Chem. Soc.*, **125**, 12420 (2003).
- H. Nishihara, *Bull. Chem. Soc. Jpn.*, **74**, 19 (2001), and references cited therein.
- M. Kurihara and H. Nishihara, *Coord. Chem. Rev.*, **226**, 125 (2002).
- M. Murata and H. Nishihara, "Metal- and Metalloid-Containing Macromolecules," ed by Caraher, Pitmanm Abd-El-Aziz, Zeldin, and Sheats, Wiley (2003), Vol. 2, Chap. 8, pp. 135–159, and references cited therein.
- M. Yamada and H. Nishihara, *Compt. Rend. Chim.*, **6**, 919 (2003), and references cited therein.
- M. Irie, *Chem. Rev.*, **100**, 1683 (2000).
- T. Ikeda and O. Tsutsumi, *Science*, **268**, 1873 (1995).
- S. Kawata and Y. Kawata, *Chem. Rev.*, **100**, 1777 (2000).
- H. Rau, "Photochromism: Molecules and Systems," ed H. Dürr and H. B.-Laurent, Elsevier, Amsterdam (1990), Chap. 4, pp. 165–192.
- H. Rau, *Angew. Chem., Int. Ed. Engl.*, **12**, 224 (1973).
- N. Tamai and H. Miyasaka, *Chem. Rev.*, **100**, 1875 (2000).
- M. Kojima, T. Takagi, and T. Karatsu, *Chem. Lett.*, **2000**, 686.
- P. P. Zarnegar and D. G. Whitten, *J. Am. Chem. Soc.*, **93**, 3776 (1971).
- P. P. Zarnegar, C. R. Bock, and D. G. Whitten, *J. Am. Chem. Soc.*, **95**, 4367 (1973).
- M.-L. Boillot, C. Roux, J.-P. Audière, A. Dausse, and J. Zarembowitch, *Inorg. Chem.*, **35**, 3975 (1996).
- V. W.-W. Yam, V. C.-Y. Lau, and L.-X. Wu, *J. Chem. Soc., Dalton Trans.*, **1998**, 1461.
- V. W.-W. Yam, Y. Yang, J. Zhang, B. W.-K. Chu, and N. Zhu, *Organometallics*, **20**, 4911 (2001).
- S. Tsuchiya, *J. Am. Chem. Soc.*, **121**, 48 (1999).
- E. C. Constable and A. M. W. C. Thompson, *J. Chem. Soc., Dalton Trans.*, **1992**, 3467.
- B. Whittle, N. S. Everest, C. Howard, and M. D. Ward, *Inorg. Chem.*, **34**, 2025 (1995).
- J.-P. Sauvage, J.-P. Collin, J.-C. Chambron, S. Guillerez, and C. Coudret, *Chem. Rev.*, **94**, 993 (1994).
- E. C. Constable and A. M. W. C. Thompson, *New J. Chem.*, **20**, 65 (1996).
- M. T. Indelli, F. Scandola, L. Flamigni, J.-P. Collin, J.-P. Sauvage, and A. Sour, *Inorg. Chem.*, **36**, 4247 (1997).
- G. D. Storrer, S. B. Colbran, and D. C. Craig, *J. Chem. Soc., Dalton Trans.*, **1997**, 3011.
- J.-P. Collin, P. Gavina, V. Heitz, and J.-P. Sauvage, *Eur. J. Inorg. Chem.*, **1998**, 1.
- J.-D. Lee, L. M. Vrana, E. R. Bullock, and K. J. Brewer, *Inorg. Chem.*, **37**, 3575 (1998).
- T. E. Janini, J. L. Fattore, and D. L. Mohler, *J. Organomet. Chem.*, **578**, 260 (1999).
- S. Kelch and M. Rehahn, *Macromolecules*, **32**, 5818 (1999).
- T. Yutaka, M. Kurihara, and H. Nishihara, *Mol. Cryst. Liq. Cryst.*, **343**, 193 (2000).

- 32 T. Yutaka, I. Mori, M. Kurihara, J. Mizutani, K. Kubo, S. Furusho, K. Matsumura, N. Tamai, and H. Nishihara, *Inorg. Chem.*, **40**, 4986 (2001).
- 33 T. Yutaka, I. Mori, M. Kurihara, N. Tamai, and H. Nishihara, *Inorg. Chem.*, **42**, 6306 (2003).
- 34 T. Yutaka, M. Kurihara, K. Kubo, and H. Nishihara, *Inorg. Chem.*, **39**, 3438 (2000).
- 35 S. R. Bohner, M. Kruger, D. Oesterhelt, L. Moroder, T. Nagele, and J. Wachtveitl, *J. Photochem. Photobiol. A: Chemistry*, **105**, 235 (1997).
- 36 M. M. J. Tecklenburg, D. J. Kosnak, A. Bhatnagar, and D. K. Mohanty, *J. Raman. Spectrosc.*, **28**, 755 (1997).
- 37 P. Hamm, S. M. Ohline, and W. Zinth, *J. Chem. Phys.*, **106**, 519 (1997).
- 38 N. Biswas and S. Umapathy, *J. Phys. Chem. A*, **104**, 2734 (2000).
- 39 P. P. Birnbaum and D. W. G. Style, *Trans. Faraday Soc.*, **50**, 1192 (1954).
- 40 S. Malkin and E. Fischer, *J. Phys. Chem.*, **66**, 2482 (1962).
- 41 D. Gegiou, K. A. Muszkat, and E. Fischer, *J. Am. Chem. Soc.*, **90**, 3907 (1968).
- 42 J. Ronayette, R. Arnaud, P. Lebourgeois, and J. Lemaire, *Can. J. Chem.*, **52**, 1848 (1974).
- 43 P. Bortolus and S. Monti, *J. Phys. Chem.*, **83**, 648 (1979).
- 44 H. Rau, *J. Photochem.*, **26**, 221 (1984).
- 45 H. Rau and S. Yu-Quan, *J. Photochem. Photobiol. A*, **42**, 321 (1988).
- 46 I. K. Lednev, T.-Q. Ye, L. C. Abbott, R. E. Hester, and J. N. Moore, *J. Phys. Chem. A*, **102**, 9161 (1998).
- 47 R. Gade and T. Porada, *J. Photochem. Photobiol. A: Chemistry*, **107**, 27 (1997).
- 48 I. K. Lednev, T.-Q. Ye, R. E. Hester, and J. N. Moore, *J. Phys. Chem. A*, **100**, 13338 (1996).
- 49 J. Wachtveitl, T. Nägele, B. Puell, W. Zinth, M. Kruger, S. R. Böhrer, D. Oesterhelt, and L. Moroder, *J. Photochem. Photobiol. A*, **105**, 283 (1997).
- 50 I. K. Lednev, T.-Q. Ye, P. Matousek, M. Towrie, P. Foggi, F. V. R. Neuwahl, S. Umapathy, R. E. Hester, and J. N. Moore, *Chem. Phys. Lett.*, **290**, 68 (1998).
- 51 J. Azuma, N. Tamai, A. Shishido, and T. Ikeda, *Chem. Phys. Lett.*, **288**, 77 (1998).
- 52 T. Yutaka, I. Mori, M. Kurihara, J. Mizutani, N. Tamai, T. Kawai, M. Irie, and H. Nishihara, *Inorg. Chem.*, **41**, 7143 (2002).
- 53 J. A. Bailey, V. M. Miskowski, and H. B. Gray, *Inorg. Chem.*, **32**, 369 (1993).
- 54 H. K. Yip, L. K. Cheng, K. K. Cheung, and C. M. Che, *J. Chem. Soc., Dalton Trans.*, **1993**, 2933.
- 55 T. K. Aldrige, E. M. Stacy, and D. R. McMillin, *Inorg. Chem.*, **33**, 722 (1994).
- 56 M. Akiba, K. Umakoshi, and Y. Sasaki, *Chem. Lett.*, **1995**, 607.
- 57 J. A. Bailey, M. G. Hill, R. E. Marsh, V. M. Miskowski, W. P. Schaefer, and H. B. Gray, *Inorg. Chem.*, **34**, 4591 (1995).
- 58 R. Büchner, J. S. Field, R. J. Haines, C. T. Cunningham, and D. R. McMillin, *Inorg. Chem.*, **36**, 3952 (1997).
- 59 G. Arena, G. Calogero, S. Campagna, L. M. Scolaro, V. Ricevuto, and R. Romeo, *Inorg. Chem.*, **37**, 2763 (1998).
- 60 D. K. Crites, C. T. Cunningham, and D. R. McMillin, *Inorg. Chim. Acta*, **273**, 346 (1998).
- 61 S.-W. Lai, M. C. W. Chan, K.-K. Cheung, and C.-M. Che, *Inorg. Chem.*, **38**, 4262 (1999).
- 62 R. Büchner, C. T. Cunningham, J. S. Field, R. J. Haines, D. R. McMillin, and G. C. Summerton, *J. Chem. Soc., Dalton Trans.*, **1999**, 711.
- 63 B. C. Tzeng, W. F. Fu, C. M. Che, H. Y. Chao, K. K. Cheung, and S. M. Peng, *J. Chem. Soc., Dalton Trans.*, **1999**, 1017.
- 64 J. F. Michalec, S. A. Bejune, and D. R. McMillin, *Inorg. Chem.*, **39**, 2708 (2000).
- 65 S. E. Hobert, J. T. Carney, and S. D. Cummings, *Inorg. Chim. Acta*, **318**, 89 (2001).
- 66 J. F. Michalec, S. A. Bejune, D. G. Cuttell, G. C. Summerton, J. A. Gertenbach, J. S. Field, R. J. Haines, and D. R. McMillin, *Inorg. Chem.*, **40**, 2193 (2001).
- 67 P. S. Zacharias, S. Ameerunisha, and S. R. Korupolu, *J. Chem. Soc., Perkin Trans. 2*, **1998**, 2055.
- 68 A. Sarkar and S. Chakravorti, *J. Lumin.*, **63**, 143 (1995).
- 69 S. Kume, M. Kurihara, and H. Nishihara, *Chem. Commun.*, **2001**, 1656.
- 70 S. Kume, M. Kurihara, and H. Nishihara, *J. Korean Electrochem. Soc.*, **5**, 189 (2002).
- 71 M.-S. Ho, A. Natansohn, C. Barrett, and P. Rochon, *Can. J. Chem.*, **73**, 1773 (1995).
- 72 M. Kurosawa, T. Nankawa, T. Matsuda, K. Kubo, M. Kurihara, and H. Nishihara, *Inorg. Chem.*, **38**, 5113 (1999).
- 73 W. P. Haret, D. W. Macomber, and M. D. Rausch, *J. Am. Chem. Soc.*, **102**, 1196 (1980).
- 74 G. C. Percy and D. A. Thornton, *J. Mol. Struct.*, **14**, 313 (1972).
- 75 J. Foley, S. Tyagi, and B. J. Hathaway, *J. Chem. Soc., Dalton Trans.*, **1984**, 1.
- 76 M. Munakata, S. Kitagawa, A. Asahara, and H. Masuda, *Bull. Chem. Soc. Jpn.*, **60**, 1927 (1987).
- 77 M. H. Al-Sayah and N. R. Branda, *Chem. Commun.*, **2002**, 178.
- 78 N. Armaroli, V. Balzani, J.-P. Collin, P. Gaviña, J.-P. Sauvage, and B. Ventura, *J. Am. Chem. Soc.*, **121**, 4397 (1999).
- 79 G. De Santis, L. Fabbrizzi, D. Iacopino, P. Pallavicini, A. Perotti, and A. Poggi, *Inorg. Chem.*, **36**, 827 (1997).
- 80 S. Kume, M. Kurihara, and H. Nishihara, *Inorg. Chem.*, **42**, 2194 (2003).
- 81 P. Federlin, J.-M. Kern, and A. Rastegar, *New J. Chem.*, **14**, 9 (1990).
- 82 A. N. Nesmeyanov, E. G. Perevalova, and T. V. Nikitina, *Dokl. Akad. Nauk SSSR*, **138**, 118 (1961).
- 83 A. N. Nesmeyanov, V. A. Sazonova, and V. I. Romanenko, *Dokl. Akad. Nauk SSSR*, **157**, 992 (1961).
- 84 M. Kurihara, T. Matsuda, A. Hirooka, T. Yutaka, and H. Nishihara, *J. Am. Chem. Soc.*, **122**, 12373 (2000).
- 85 W. H. Morrison, Jr., S. Krogsrud, and D. N. Hendrickson, *Inorg. Chem.*, **12**, 1998 (1973).
- 86 H. Nishihara, *Adv. Inorg. Chem.*, **53**, 41 (2002).
- 87 K. M. Omberg, P. Y. Chen, and T. J. Meyer, *Adv. Chem. Phys.*, **106**, 553 (1999).
- 88 S. Brunschwig, C. Creutz, and N. Sutin, *Coord. Chem. Rev.*, **177**, 61 (1998).
- 89 C. Creutz, M. D. Newton, and N. Sutin, *J. Photochem. Photobiol. A: Chem.*, **82**, 47 (1994).
- 90 S. Korupolu, M. Kurihara, and H. Nishihara, in preparation.
- 91 M. Kurihara, A. Hirooka, S. Kume, M. Sugimoto, and H. Nishihara, *J. Am. Chem. Soc.*, **124**, 8800 (2002).
- 92 J. A. McCleverty, *Prog. Inorg. Chem.*, **2**, 72 (1969).
- 93 R. P. Burns and C. A. McAulliffe, *Adv. Inorg. Chem. Radiochem.*, **22**, 303 (1979).
- 94 M. Fourmigue, *Coord. Chem. Rev.*, **178–180**, 823 (1998).

- 95 H. Nishihara, M. Okuno, N. Akimoto, N. Kogawa, and K. Aramaki, *J. Chem. Soc., Dalton Trans.*, **1998**, 2651.
- 96 A. Sugimori, T. Akiyama, M. Kajitani, and T. Sugiyama, *Bull. Chem. Soc. Jpn.*, **72**, 879 (1999).
- 97 M. Nihei, T. Nankawa, M. Kurihara, and H. Nishihara, *Angew. Chem., Int. Ed.*, **38**, 1098 (1999).
- 98 M. Nihei, M. Kurihara, J. Mizutani, and H. Nishihara, *Chem. Lett.*, **2001**, 852.
- 99 M. Nihei, M. Kurihara, J. Mizutani, and H. Nishihara, *J. Am. Chem. Soc.*, **125**, 2964 (2003).
- 100 J. Darkwa, *Inorg. Chim. Acta*, **257**, 137 (1997).
- 101 K. G. Landis, A. D. Hunter, T. R. Wagner, L. S. Curtin, F. L. Filler, and S. A. Jansen-Varunum, *Inorg. Chim. Acta*, **282**, 155 (1998).
- 102 Ş. Işık, S. Öztürk, H.-K. Fun, E. Agar, and S. Şaşmaz, *Acta Crystallogr., Sect. C*, **56**, 95 (2000).
- 103 C. Handrosch, R. Dinnebier, G. Bondarenko, E. Bothe, F. Heinemann, and H. Kish, *Eur. J. Inorg. Chem.*, **1999**, 1259.
- 104 G. V. Boyd, T. Norris, P. F. Lindley, and M. M. Mahmoud, *J. Chem. Soc., Perkin Trans. 1*, **1977**, 1612.
- 105 G. V. Boyd, T. Norris, and P. F. Lindley, *J. Chem. Soc., Perkin Trans. 1*, **1977**, 965.
- 106 G. A. Bowmaker, P. D. W. Boyd, and G. K. Campbell, *Inorg. Chem.*, **21**, 2403 (1982).
- 107 A. M. Bond and V. Tedesco, *Inorg. Chem.*, **33**, 5761 (1994).
- 108 S. P. Kaiwer, A. Vodacek, N. V. Bloufh, and R. S. Pilato, *J. Am. Chem. Soc.*, **119**, 3311 (1997).
- 109 S. P. Kaiwer, J. K. Hsu, A. Vodacek, G. Yap, L. M. Liable-Sands, A. L. Rheingold, and R. S. Pilato, *Inorg. Chem.*, **36**, 2406 (1997).
- 110 S. P. Kaiwer, A. Vodacek, N. V. Blough, and R. S. Pilato, *J. Am. Chem. Soc.*, **119**, 9211 (1997).
- 111 N. Nishimura, S. Kosako, and Y. Sueishi, *Bull. Chem. Soc. Jpn.*, **57**, 1617 (1984).
- 112 N. Nishimura, T. Sueyoshi, H. Yamanaka, E. Imai, S. Yamamoto, and S. Hasegawa, *Bull. Chem. Soc. Jpn.*, **49**, 1381 (1976).
- 113 T. Sueyoshi, N. Nishimura, S. Yamamoto, and S. Hasegawa, *Chem. Lett.*, **1974**, 1131.
- 114 J. Anzai and T. Osa, *Tetrahedron*, **50**, 4039 (1994).



Hiroshi Nishihara was born in 1955 in Kagoshima Prefecture, Japan. He received his B. Sc. degree in 1977, M. Sc. in 1979 and D. Sc. in 1982 from The University of Tokyo. He was appointed research associate of Department of Chemistry, Faculty of Science and Technology at Keio University in 1982, and he was promoted lecturer in 1990, and associate professor in 1992. Since 1996, he has been a professor of Department of Chemistry, School of Science at The University of Tokyo. He also worked as a visiting research associate in the Prof. Royce W. Murray's group of Department of Chemistry at The University of North Carolina at Chapel Hill (1987–1989), and as a researcher of PRESTO, JRDC (1992–1996). His research has been focused on creation of new electronically and optically functional materials comprising both transition metals and π -conjugated chains, and invention of unidirectional electron transfer systems utilizing molecular layer interfaces.